Received: 13 March 2023 | Accepted: 17 April 2023

DOI: 10.1002/pgr2.4

COMPREHENSIVE REVIEW

Proteoglycan Research WILEY

Functional organization of extracellular hyaluronan, CD44, and RHAMM

Mary K. Cowman[1,2] | **Eva A. Turley**[3,4,5,6]

[1]Department of Biomedical Engineering, Tandon School of Engineering, New York University, New York, New York, USA

[2]Department of Orthopedic Surgery, Grossman School of Medicine, New York University, New York, New York, USA

[3]London Regional Cancer Program, London Health Sciences Centre, Lawson Health Research Institute, London, Ontario, Canada

[4]Department of Oncology, Schulich School of Medicine and Dentistry, Western University, London, Ontario, Canada

[5]Department of Biochemistry, Schulich School of Medicine and Dentistry, Western University, London, Ontario, Canada

[6]Department of Surgery, Schulich School of Medicine and Dentistry, Western University, London, Ontario, Canada

Correspondence

Mary K. Cowman, Department of Biomedical Engineering, Tandon School of Engineering, New York University, 433 First Ave, New York, NY 10010, USA.
Email: mary.cowman@nyu.edu

Eva A. Turley, London Regional Cancer Program, London Health Sciences Centre, Lawson Health Research Institute, Room A4-931A, 790 Commissioners Rd East, London, ON N6A 4L6, Canada.
Email: eva.turley@lhsc.on.ca

Funding information

Lawson Health Research Institute; Cancer Research Society

Abstract

The integral membrane protein CD44 is constitutively expressed in most tissues, and is the primary cell surface receptor for hyaluronan (HA). HA is the key scaffolding organizer of proteoglycans and receptors in the extracellular matrix. CD44 is expressed as cell type-specific and context-specific alternatively spliced isoforms with variable glycosylation and interreceptor interactions. CD44 plays a critical role in the organization and patterning of domains in the cell membrane, achieved through linking the cortical actin cytoskeleton with the pericellular HA matrix. This functional and spatial organization of CD44 and HA maintains a protective and homeostatic cellular microenvironment. Tissue injury and cellular stress result in HA fragmentation and unconventional export of the CD44 coreceptor, RHAMM, which collectively alter the homeostatic organization of CD44/HA. The resulting interplay among HA, HA fragments, CD44 and RHAMM triggers cellular responses such as cell motility that contribute to tissue repair, and disease processes. Here we review current understanding of the structural biology of HA, CD44, and RHAMM, and provide an overview of their known functional organization and patterning at the cell surface. Changes in their surface organization act as sensors for detecting

Abbreviations: aa, amino acid; ADAM10, a disintegrin and metalloproteinase domain-containing protein 10; ADAM17, a disintegrin and metalloproteinase domain-containing protein 17; AFM, atomic force microscopy; AURKA, Aurora Kinase A; BRET, bioluminescent resonance energy transfer; CD44, cluster of differentiation protein 44; CD44H, CD44s, CD44 hematopoietic, standard form; CS, chondroitin sulfate; Da, Dalton; E2F1, E2F transcription factor 1; ECD, extracellular domain; EGFR, epidermal growth factor receptor; ER, endoplasmic reticulum; ERM, ezrin, radixin, moesin; FL-HA, fluorescent HA; FRET, fluorescence resonance energy transfer; G2M, G2-M DNA damage checkpoint in the mitotic cycle; GFP, green fluorescent protein; GlcA, glucuronic acid; GlcNAc, N-acetyl glucosamine; HA, hyaluronan; HABD, hyaluronan-binding domain; HAS, hyaluronan synthase; HC, heavy chain of inter-α-inhibitor; HMMR, hyaluronan mediated motility receptor; HMW, high molecular weight; HS, heparan sulfate; ICD, intracytoplasmic domain; IGD, interglobular domain; KS, keratan sulfate; LMW, low molecular weight; MAP kinase, mitogen-activated protein kinase; MMP9, matrix metalloproteinase 9; MMW, medium molecular weight; MT1-MMP, membrane-type 1 matrix metalloproteinase; MW, molecular weight; Ni-NTA, nickel nitrilotriacetic acid; NMR, nuclear magnetic resonance; PCM, pericellular matrix; PDGFR, platelet-derived growth factor receptor; PG, proteoglycan; PKC, protein kinase C; PMA, TPA, phorbol 12-myristate 13-acetate; RHAMM, receptor for hyaluronan-mediated mobility; RNS, reactive nitrogen species; RON, Recepteur d'Origine Nantais; ROS, reactive oxygen species; RUNX2, Runt-related transcription factor 2; SDS-PAGE, sodium dodecyl sulfate polyacrylamide gel electrophoresis; SPR, surface plasmon resonance; TEM, transmission electron microscopy; TGFBR1, transforming growth factor beta receptor 1; TLR, Toll-like receptor; TM, transmembrane; TSG-6, tumor necrosis factor-stimulated gene 6 protein; ZSGP, Zoanthus sp. green fluorescent protein.

danger, and are critical to the understanding of consequent intracellular signaling and response mechanisms to cellular stress.

KEYWORDS
CD44, extracellular matrix, hyaluronan, pericellular matrix, RHAMM

INTRODUCTION

The Fluid Mosaic Membrane model was proposed in 1972 as a nanoscale template for the organization of the plasma membrane.[1] New techniques and increased depth in understanding of cell–cell and cell–matrix interactions as well as organizational principles have expanded this original view of a largely fluid plasma membrane into one of a fluid but densely packed mosaic structure. This structured organization results in the creation of dynamic cell surface domains with distinct mobilities, surface half-lives, which therefore differentially input intracellular, spatially compartmentalized, signaling cascades.[1] During homeostasis, this complex and dynamic patterning appears to function in a highly coordinated manner, which is disrupted with disease.[2] This complexity provides enormous potential for functional diversity and context-dependent responses. Identifying the proteins, proteoglycans (PG), and glycans that are key organizers of cell membrane patterning will not only increase our knowledge of how cells sense and response to their microenvironment but also provide new therapeutic approaches to managing disease. The HA receptors, CD44 and RHAMM are examples of proteins that affect the spatial organization of the plasma membrane that notably affect cell migration during responses-to-injury.[3–7]

Here, we focus on the structure and properties of hyaluronan (HA), CD44, and RHAMM (*HMMR*), that mediate mutual interactions controlling their clustering and patterning at the cell surface. These interactions constitute a critical cellular sensing mechanism, which is central to the detection of danger and which contributes to an initial response to tissue stress.[8–10] The cell surface microarchitecture resulting from these HA: HA receptor interactions provides an interface between the pericellular milieu and the intracellular cytoskeleton/signaling complexes that is particularly sensitive to ROS/RNS levels, which cleave the native HA polymer. HA fragmentation and the unconventional export or extracellular release of RHAMM that occurs with cellular stress[11,12] modifies CD44 patterning from its homeostatic microarchitecture, and initiates signaling pathways contributing to a response-to-injury and disease.[3,13] The signaling pathways that are activated by these changes, which include the Toll-like receptor (TLR)-mediated inflammasome,[8,14] MAP kinase pathways, and AURKA/centrosome signaling,[11,15] control cytoskeleton remodeling, gene transcription and other cellular responses (e.g., cell survival/death and migration) are required for an effective response-to-injury. We do not cover these signaling responses or their deregulation that leads to disease since they have been addressed by excellent reviews.[15–22]

HA

HA, also called hyaluronic acid, is a linear glycosaminoglycan polymer composed solely of repeating disaccharides of [(1→3)-β-D-GlcNAc-(1→4)-β-D-GlcA].[23,24] HA is synthesized by three integral membrane HA synthase enzymes, HAS1, HAS2, and HAS3, and is extruded directly to the pericellular space.[25–27] The termination step in HA synthesis is not understood, but the HA produced by any of the three synthase enzymes appears to be polydisperse in size. While the covalent sequence of HA is invariant in nature, the molecular weight (MW) can vary over a wide range.[28] The average molecular weight of HA in healthy tissues (e.g., young human cartilage, human skin, human vitreous, human synovial fluid, rabbit skin, rat skin, rooster combs, rabbit skeletal muscle, lung, heart, ileum, colon) is commonly 2000–6000 kDa.[29–37] In other human fluids such as milk, amniotic fluid, lymph, blood, saliva, and urine, and in solid tissues that are aging, irradiated, inflamed, wounded, or cancerous, the average MW is generally lower, and the range of sizes present can include short HA fragments.[32,35,38–47] There is no consensus in the literature on the definitions for high molecular weight (HMW) or low molecular weight (LMW) HA. Here, we will refer to HA with an average MW of >500 kDa as HMW, and HA with an average MW of <100 kDa as LMW. Medium MW (MMW) HA, 100–500 kDa, has physicochemical properties that are fundamentally similar to HMW HA, but its presence in vivo can indicate ongoing degradative or remodeling processes that also yield LMW HA.

HA conformation and crowding effects

The conformation, flexibility, and mutual crowding of HA molecules in solution have been reviewed previously, and are briefly described here.[48,49] X-ray fiber diffraction analyses of HA in stretched membranes show extended rope-like helical conformations with 2, 3, or 4 disaccharides per turn of helix, and projected length of a disaccharide unit along the helix axis of 0.85–0.95 nm for sodium salt forms, which is close to the maximum projected length of 1 nm (Figure 1).[50–53] In the solid state, each glycosidic linkage is stabilized by hydrogen bonds, but NMR studies of HA show that the hydrogen bonds are dynamically formed and broken in aqueous solution, allowing segmental motions on a nanosecond time scale.[54–58] The molecular shape of HA in dilute aqueous solutions has been characterized as a wormlike coil with a persistence length of 4–5 nm by hydrodynamic methods, including viscosity, light scattering, and sedimentation-diffusion.[48,59–68] Due to charge repulsion

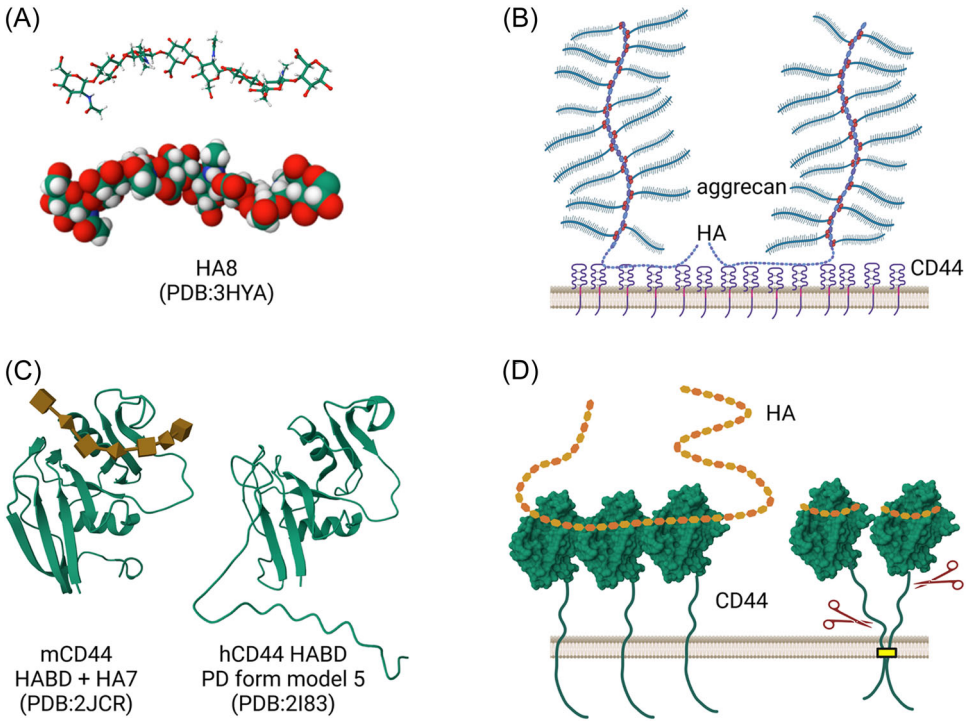

FIGURE 1 HA, aggrecan, and CD44 interact at the cellular surface. (A) HA octasaccharide (HA8) shown in skeletal and space-filling models based on the structure determined by X-ray fiber diffraction. From PDB ID 3HYA (https://doi.org/10.2210/pdb3HYA/pdb), (Guss et al.[50]). (B) HA is tethered to integral membrane protein CD44, and binds multiple aggrecan proteoglycans to create a pericellular matrix. (C) The HA-binding domain (HABD) of murine CD44 (crystal structure with HA8, 7 crystallographically determined residues) (PDB ID 2JCR at rcsb.org) and a representative NMR-derived structure (model 5 of 20) for the partially disordered (PD) human CD44 HABD (PDB ID 2I83 at rcsb.org), illustrating the increased disorder in the flexible C-terminal segment when bound to HA in solution. PDB ID 2JCR (https://doi.org/10.2210/pdb2JCR/pdb), S. Banerji, A. J. Wright, M. E. M. Noble, D. J. Mahoney, I. D. Campbell, A. J. Day, D. J. Jackson. *Nat. Struct. Mol. Biol.* **2007**, *14*, 234. PDB ID 2I83 (https://doi.org/10.2210/pdb2I83/pdb), M. Takeda, S. Ogino, R. Umemoto, M. Sakakura, M. Kajiwara, K.N. Sugahara, H. Hayasaka, M. Miyasaka, H. Terasawa, I. Shimada. *J. Biol. Chem.* **2006**, *281*, 40089. (D) HMW HA and HA fragments bind clustered CD44 and CD44 dimers, which can be disulfide-linked at C286 in the TM domain. Sites for enzymatic cleavage by MT1-MMP (G192, close to the HABD) or ADAM protease (S249, close to the TM domain) are indicated. The CD44 HABD structure is PDB ID 2JCR. All PDB structures were accessed on the RCSB PDB (rcsb.org), and visualized with Mol* software (D. Sehnal, S. Bittrich, M. Deshpande, R. Svobodová, K. Berka, V. Bazgier, S. Velankar, S. K. Burley, J. Koča, A. S. Rose. *Nucleic Acids Res.* **2021**. https://doi.org/10.1093/nar/gkab314). Figure created with BioRender.com.

between the carboxyl groups and limited conformational flexibility resulting from steric hindrance at the glycosidic linkages, short HA chains have extended, almost rod-like, conformations, while HA chains greater than about 40 kDa in MW adopt a range of randomly coiled shapes that average over time to an approximately spherical (but not impenetrable) domain. Because of that inherent chain semi-flexibility, the effective volume occupied by a single HA molecule is very large, even though most of the space is actually occupied by water and counterions. The volume of the HA molecular domain is also a strong function of the HA molecular weight. While the volume of a compactly folded globular protein increases in direct proportion to its molecular weight, the volume of a loosely coiled HA chain increases almost as the square (more precisely, $M^{1.8}$) of the molecular weight. For HA with a molecular weight of 3000 kDa, corresponding to a chain length of 7500 nm, the equivalent spherical space occupied by a single chain would have a diameter of about 400 nm. At a high enough concentration that the HA coils start to touch (about 570 μg/mL for 3000 kDa HA), the physical properties of the solution change dramatically. Each chain causes its neighbors to have less available space, and a higher effective concentration. This mutual macromolecular crowding is the basis for the extraordinary high viscosity and elasticity of HMW HA solutions.[49,69–75]

HA has the ability to self-associate. A double helix form was observed by X-ray fiber diffraction studies, in the presence of Cs^+, Rb^+, NH_4^+, or mixed K^+/H^+ counterions.[76,77] In physiological aqueous NaCl solution, intermolecular association was detected for short chains containing about 14–80 monosaccharides (HA14-80; 2.8–16 kDa) but not for longer HA, when studied at concentrations greater than 1 mg/mL.[48,66] When HA is deposited on solid surfaces and imaged by transmission electron microscopy (TEM) or atomic force microscopy (AFM), self-association can lead to a wide variety of forms with intramolecular hairpins, pearl necklace, and rod-like condensation, and intermolecular network formation. Such associated forms are very commonly observed for both HMW and LMW HA, whereas uncoiled single chains are relatively difficult to image unless trapped within a thin layer of ordered water on a hydrophilic

surface.[78–82] Because surface immobilization of HA can lead to self-association unless the attachment is specific and at low density (e.g., attachment via a unique end label), due care must be exerted in studies of surface-bound HA in interaction with binding proteins or cells.

HA in the extracellular and pericellular matrix

In the extracellular matrix, HA, fibrillar proteins, PG, globular proteins, and small molecules are present simultaneously. Intermolecular binding interactions control the organization. In addition, crowding by these macromolecules has the effect of reducing available space. Mobile proteins partition (distribute) preferentially to spaces with fewer restrictions to movement. HA contributes to this effect, acting like a gel filtration network that tends to exclude proteins based on their size relative to the open spaces in the network between segments of HA chain, dictated by the HA concentration. As a pioneer of this concept and the physical chemistry of HA, Torvard Laurent provided the quantitative theory for this effect, and showed that it correctly predicts the tendency of proteins to distribute preferentially to low-concentration HA spaces relative to high-concentration HA spaces.[83,84]

In the pericellular matrix (PCM), newly synthesized HA chains may remain attached to the synthase enzyme, while released HA chains can be tethered to the cell surface by integral membrane receptor proteins, the most widely distributed being CD44. The microenvironment surrounding HA in the pericellular matrix also contains secreted proteins and PG that can specifically bind HA and control its organization. There is significant variation in the composition of the PCM among tissues, and as a function of the physiological state.

HA-binding PG such as aggrecan and versican in the PCM promote the formation of a highly expanded and hydrated cell coat.[85–87] The structure and organization of aggrecan in the HA extracellular matrix of cartilage and in the PCM of chondrocytes has been characterized in detail. Aggrecan has a protein core with an N-terminal globular G1 domain, a short extended interglobular domain (IGD), a second G2 globular domain, followed by a longer extended protein domain with covalently attached keratan sulfate and chondroitin sulfate glycosaminoglycan chains, and a C-terminal G3 domain. The protein also has variable glycosylation with N- and O-linked oligosaccharides. The proteoglycan structure resembles a bottle brush. A single aggrecan chain can have a molecular weight of approximately 2500 kDa, depending on the number and length of the attached glycan chains. Aggrecan PG bind noncovalently to HA through the G1 domain. This binding interaction is strongly stabilized by the small cartilage link protein, HAPLN1, via a structure homologous to aggrecan G1, which binds to both HA and the aggrecan. A single HA chain can bind a large number of aggrecan PG, creating assemblies that fill much of the pericellular space.

The ability of the PCM to control the equilibrium distribution and mobility of other macromolecules near the cell surface depends on the content and structural organization of HA and PG, with HA being the key controlling component.[86,88–90] The best characterized PCM structure is that of cultured chondrocytes. A single HA chain can bind to multiple CD44 receptors, and can simultaneously bind and assemble PG such as aggrecan and versican (Figure 1). While HA without bound PG would occupy a loosely coiled conformation as described above, the binding of large PG molecules straightens and extends HA chains to accommodate the crowding between PG, as well as the electrostatic repulsion due to sulfated glycosaminoglycan chains.[91–93] The PCM thus develops into an expanded meshwork of HA-PG assemblies. The maximum size of the PCM is dependent on the HA length and on the content of attached PG, as well as the presence of plasma membrane microvilli, which provide scaffolding that expands the PCM, even if the PG content is low.[85] The region of the PCM that is closest to the cell surface is denser, more elastic, and has a smaller mesh size, which restricts macromolecular movement and partitioning. The PCM is progressively more open further from the cell.[92–94] Despite the crowding, tethered HA chains and attached PGs create a viscoelastic medium, retaining the ability to move, and are not crosslinked significantly on cultured chondrocytes.[91,92,95] In vivo, depending on the cell type and functional status, HA-PG assemblies can be crosslinked via protein-mediated crosslinking of PG G3 domains. Under inflammatory conditions, HA can also be crosslinked by upregulated TSG-6 and its binding proteins, or by self-association of protein heavy chains (HC) derived from inter-α-inhibitor, covalently transferred to HA by TSG-6.[85,96]

Homeostasis in the PCM depends on coordinated synthesis and degradation. Such coordination of HA and aggrecan synthesis and degradation has been demonstrated in bovine cartilage organ cultures[97] In contrast, injury and disease in many tissues can cause dysregulation of HA/PG synthesis and degradation.[86] Proteolytic degradation of PGs, and extracellular hyaluronidase activity both disrupt the PCM.[98–105] HA is also highly susceptible to degradation by reactive oxygen and nitrogen species.[49,106,107] Increased HA synthesis and degradation are commonly associated with inflammation and cancer.[108–113]

HA size-dependent effects

In general, HMW HA is associated with healthy tissue. Purified HMW HA is anti-inflammatory, nonantigenic, linked to cancer resistance and has numerous medical applications.[114–118] However, synthesis and buildup of excess HA can be associated with poor prognosis in many cancers,[111,119] and impaired lung function in COVID-19 patients.[120,121] However, LMW-HA and HA oligosaccharides that are present in diseases are generally not detected in heathy tissues. These promote inflammation and support invasion.[8,122–129] HA/receptor interactions that require HMW can be disrupted by competition with fragments, with a resulting loss of normal signaling. Additional inflammatory response to LMW HA can arise when it is detected as a danger signal by activation of TLRs. Because the expression of innate immune receptors depends on the tissue type

and status, the response to HA fragments can be highly variable. As well several reports have identified conditions where HA fragments are not proinflammatory if free of endotoxins,[130–134] and that fragments can be generated in the body by medical use of recombinant hyaluronidase without causing inflammation.[135] Specific sizes of HA fragments can even be therapeutic by stimulating defensive and remodeling responses.[136,137] Clearly, our understanding of the function of specific sizes of LMW-HA and HA oligosaccharides is currently incomplete.

In this review, we focus on the molecular aspects of extracellular interactions between HA, CD44, and RHAMM, and note conditions under which HA size may affect those interactions.

CD44 INTERACTION WITH HA AS A DETERMINANT OF CELL SURFACE PATTERNING

CD44 is the key HA receptor protein that is constitutively expressed and responsible for contributing to multiple HA-dependent cellular processes, including cell–cell adhesion, cell migration, lymphocyte homing, and leukocyte activation.

Initial findings regarding the fundamental parameters of HA-CD44 binding came from studies of HA-dependent intercellular adhesion of murine SV40-3T3 and other cell lines.[138–143] The then-unidentified receptor was found to be a protein susceptible to cleavage by trypsin that bound HA fragments with a minimum length of six monosaccharides (HA6). Polymeric HA showed molecular weight-dependent affinity for this protein that was later identified as CD44. The receptor responsible for SV40-3T3 cell–cell interaction was detected by a monoclonal Hermes antibody prepared against the human CD44 lymphocyte homing receptor, providing the first evidence that CD44 is an HA receptor.[144] CD44 was subsequently shown to be constitutively expressed in most tissues and in multiple types of cells, including smooth muscle cells, skin epithelial cells, and chondrocytes,[145] and to anchor the pericellular matrix, which is scaffolded by HA and HA-associated proteins (aggrecan, versican, and HAPLN1 link protein), to cells.[86,88,89] This pericellular matrix is removed from CD44 by competitive binding of HA hexasaccharides,[146] confirming the identity of CD44 as an HA receptor and setting the stage for parsing the differential effects of HA polymer sizes on cell function and organization of membrane domain structure.

CD44 gene and protein domain structure

The gene for CD44 protein contains 20 exons.[147–151] It can be expressed as multiple different isoforms generated by alternative splicing and extensive posttranslational modification.[18,152] Exons 1–5 encode a highly conserved extracellular domain found in all CD44 proteins. Exons 6–15 encode membrane proximal domains found in its variant forms (v1–v10). Exons 16 and 17 comprise the constant membrane-proximal domain. Exon 18 encodes the transmembrane domain common to all isoforms. The short exon 19 and a much longer exon 20 are alternative sequences encoding the intracellular domain.

CD44s, the "standard" form of CD44, is widely distributed and has also been referred to as CD44H, based on its discovery in hematopoietic cells. CD44s lacks all sequence encoded in the extracellular variant exons, and is translated from exons 1–5, 16–18, and 20. CD44s is typically expressed by cells of mesenchymal origin. Variant forms of CD44 are typical of cells of epithelial origin, for example, CD44v3-v10 expressed by keratinocytes encodes eight of the variable membrane proximal exons. Tumors arising from parenchyma express multiple CD44 variants.

As a type I transmembrane protein, CD44s contains a 20 amino acid (aa) signal peptide sequence followed by 341 amino acids of the mature protein. The protein has three domains: an extracellular domain of 248 aa (ECD), a 21 aa transmembrane domain (TM), and a 72 aa intracellular domain (ICD). The molecular weight of this protein core is 37 kDa, but its sodium dodecyl sulfate polyacrylamide gel electrophoresis (SDS-PAGE) mobility corresponds to an apparent molecular weight of 80–90 kDa, resulting from extensive glycosylation.[153,154] For example, in humans, there are six (five in mouse) conserved sites for potential N-glycosylation and multiple potential sites for O-glycosylation in the ECD alone.[155]

Functionally, the ECD of CD44s binds HA in a glycosylation- and disulfide bond reduction-dependent manner, and the ICD has several functions. It connects CD44 to the actin cytoskeleton in a phosphorylation-dependent interaction with ERM proteins (ezrin, radixin, moesin), ankyrin, and merlin (NF2) that impacts cell adhesion and motility (see CD44-cytoskelton section below). The ICD, which can be released by gamma secretases, also participates in transcriptional complexes (e.g., RUNX2) to regulate genes linked to proliferation and motility, such as MMP9. The TM domain includes a cysteine residue, which can be palmitoylated, driving partition of CD44 into lipid rafts.[156,157] Each of these domains can also participate in interactions that lead to nanoscale homodimerization (e.g., by disulfide bond formation) and oligomerization (clustering) of CD44, which contribute to the heterodimerization with other receptors.

CD44 variants differ in molecular weight due to the added sequence in the membrane-proximal portion of the ECD. They also carry additional glycosylation at multiple potential acceptor sites. Particularly impactful O-glycosylation can include attachment of heparan sulfate (HS), chondroitin sulfate (CS), or keratan sulfate (KS), thus expanding the binding partners available to CD44. For example, decoration of CD44 with CS provides fibronectin, laminin, and collagen-binding functionality, while HS attachment provides binding sites for growth factors and chemokines.[158,159]

Structure of the CD44 HA-binding domain (HABD)

The HABD occupies the first 158 amino acids (numbered 21–178, counting from the start of the cleaved signal peptide). Residues 32–124 constitute a "Link module" that is homologous to the HABD of TSG-6, aggrecan, versican, HAPLN1, and LYVE1.

Site-directed mutagenesis identified specific CD44 residues that are required for HA binding. Several studies indicate that most of the critical aa for HA binding occur within the CD44 Link module. Thus, Peach et al.[160] used a CD44 ECD (21–220aa)-IgG fusion protein to show that site mutation of R29, K38, and R41 to Ala significantly reduces HA binding with R41 being the most important. Mutation of R150, R154, K158, and R162 to Ala, which are not part of the Link module, also reduces binding to HA but to a lesser extent. Bajorath et al.[161] employed a full length CD44s-IgG2a fusion protein to show that site-directed mutation of K38, **R41**, **Y42**, K68, **R78**, **Y79**, N100, N101, and Y105 to Ala significantly inhibits HA binding, with residues in bold being critical. Molecular modeling of the CD44 Link module (aa32–123) predicts a similar conformation to the NMR-derived TSG-6 Link module, whose folded structure is stabilized by two disulfide bonds.[161] NMR and X-ray crystallography studies by Jackson, Day, and coworkers.[162] using unglycosylated, recombinant CD44 HABD (aa20–178) showed that residues 20–169 form a compactly folded structural domain, while residues 170–178 are more disordered. The Link module portion (aa32–124) of HABD is compactly folded as two α helices and two three-stranded β sheets similar to TSG6. However, the entire CD44 HABD (aa21–178) contains a β sheet that extends from the Link module adding four additional β strands. Essentially, the N-terminal extension of residues 21–31, and the C-terminal extension of residues 125–178, fold to form an additional lobe in the HABD of CD44 that is not present in the TSG-6 HABD. A third disulfide bond links these extensions at aaC28 and C129.

A model for HA binding to CD44 was deduced by NMR using an HA octasaccharide (HA8) bound to unglycosylated, recombinant HABD.[162] Two possible paths for initiating HA binding to the HABD surface were proposed, and conformational changes resulting from HA binding to the relative orientation between the Link module and the rest of the HABD sequence were predicted. One path of binding requires K38 and R162 while the second path utilizes R150 and R154 but both paths require R41, Y42, R78, and Y79. The HA octasaccharide (HA8) fills either path. Glycosylation of N25, which is spatially close to R150 and R154, is speculated to dictate the path chosen for HA binding. The opposite face of the HABD also has several residues that have been identified by site-directed mutation[163] to contribute to HA binding, including N120 which may function indirectly by inhibiting CD44 self-association when glycosylated.[162]

Unglycosylated, recombinant mouse CD44 HABD (aa25–174) was successfully crystallized as a complex with HA8 that reveals two different structures, denoted as type A and B.[164] Type A is similar to the crystal structure of HABD without HA8 while type B conformation (Figure 1) of HABD/HA8 is shifted from the unbound structure near the β1-α1 loop. However, both structures predict only a shallow groove for HA binding although type B provides higher binding affinity. The nonreducing terminal GlcA of HA8 is not restricted by CD44 binding, and significant contacts are primarily with GlcA at the fifth residue position (counting from the nonreducing end) and GlcNAc at the eighth residue (i.e., the reducing end) of HA8. Binding of HA8 to HABD also results in a kinked conformation between GlcA (5) and GlcNAc(6) and is primarily stabilized by a combination of hydrogen bonds, hydrophobic interactions, and van der Waals interactions. It does not appear to be significantly stabilized by electrostatic and CH–π interactions predicted by the interactions of HA8 with TSG-6. This is consistent with the observed increased binding of HA to CD44 in the presence of 0.5 M NaCl. All of the stabilizing interactions occur within the Link module, and are not contributed to by the R and K residues in the outer HABD lobe formed by the N- and C-terminal extensions. Lack of involvement of these aa in binding to HMW-HA was confirmed by site mutation when binding affinity is measured by SPR, or inferred by NMR conformation and binding of fluorescently labeled HMW-HA to cells. These data predict the CD44 HABD conformation changes from type A to B upon HA8 binding, due to movement of a loop containing R45 (= R41 in human CD44), providing a closer fit to HA. N-deglycosylation of the native HABD is speculated to favor the same conformational change to the higher affinity binding type B.[164]

A modified model for CD44 that involves a significant change in conformational flexibility upon binding to HA was proposed by Shimada and coworkers[165] on the basis of NMR studies of the human recombinant CD44 HABD (residues 21–178) bound to HA34. The major protein residues exhibiting change upon HA binding are located outside the Link module of the HABD. Similarly, an NMR study of HA6 bound to this recombinant CD44 HABD indicate a conformational change that partially disorders the outer region.[166] Two interconverting HABD conformations are proposed.[167] In a more ordered "O" form, the N- and C-termini of HABD extending outside of the link module appear closely folded to the Link module as a second lobe. In the more open and relaxed, partially disordered "PD" conformation, the C-terminal extension is no longer closely folded on the Link module (Figure 1). The equilibrium between the two CD44 HABD conformations is proposed to explain the apparent inconsistency between structures deduced from NMR data and X-ray crystallography. Thus, crystallization with or without HA binding favors the more compact ordered "O" form. Further solution state binding studies of a mutant CD44 HABD locked into the "PD" relaxed form show it has higher HA binding affinity than the "O" form, and cells transfected with a stabilized PD form are less efficient in rolling (i.e., are more tightly bound) on an HA surface under flow conditions.[167]

In further support of the model in which HA binding induces an opening of the CD44 HABD conformation and increases flexibility of the C-terminal extension, molecular dynamics simulations support an order-disorder transition of aa 153–169.[168,169] This allows significant segmental motion, such that R154, K158, and R162 can move to make closer contact with the bound HA chain, creating transient binding, with R154 being most involved. (Note that R154 had been identified as a contributor to binding affinity in early site-directed mutation analyses[160]).

When the binding of HA to cell surface CD44 results in applied force, as exists in the presence of high shear blood flow, the potential for flexibility in the CD44 HABD structure allows a mechanosensitive

conformational switch between low- and high-affinity states in the C-terminal extension β8/β9 strands of the HABD.[170] In accord with this model, 10 μm beads coated with CD44 HABD show evidence of a shear stress-induced unfolding of the C-terminal region, leading to increased HA-binding affinity.[171] Molecular dynamics simulations suggest that force-induced extension of the C-terminal extension can then trigger a further change in the PD form, refolding into a more compact arrangement with greater affinity for HA, although experimental data have not yet confirmed this.[172]

The in vivo CD44 HABD structure has additional layers of complexity that modulate HA binding affinity since it is glycosylated in a cell type- and context-dependent manner. N-glycosylation, especially with terminal sialic acid, significantly inhibits HA binding by blocking high-affinity sites on the CD44 Link module surface,[163,173,174] and sialidase activity removes this inhibition.[175,176] HA binding affinity is also modified by redox status. Within the Link module, reduction of the labile disulfide bond linking C77 with C97, which lies in the shallow binding groove of the Link module, inhibits HA binding. The C53–C118 disulfide linkage is buried in the core and not susceptible to reduction. In the added lobe formed by the N- and C-terminal extensions, the disulfide bond linking C28–C129 is predicted to be labile, and thus may dynamically influence the nature and extent of conformational change associated with HA binding. These data show that factors affecting both glycosylation and redox status can actively tune CD44-HA binding affinity.[177]

HA binding affinity depends on CD44–CD44 interactions (and vice versa)

Nanoscale (molecular level) self-association of CD44 molecules has a significant effect on both its binding affinity for HA, and dependence on HA molecular weight. CD44 isolated from SV40-3T3 cells binds to oligosaccharides as small as HA6 but the isolated receptor has lower affinity for HA than on intact cells, and does not display binding preference for HMW HA.[143] One explanation for this discrepancy is that the binding of HA to CD44 embedded in a cell membrane is multivalent, and based on coordinate binding of polymeric HA by multiple CD44 proteins (Figure 1), whereas isolated receptors offer only monovalent binding. This concept is supported by experiments of fluorescently labeled HA (FL-HA) binding to intact cells, where the minimum size of HA oligosaccharide that blocks FL-HA is HA6, while HA10 and HA20+ bind with increasing affinity.[178] Other reports show that CD44 clustering enhances HA-binding affinity more directly. For example, depending on the glycosylation status of CD44, $CD44^{+}$_cells can be induced to bind HA by anti-CD44 antibody-induced dimerization.[179–181] CD44 dimer formation is stabilized by a disulfide bridge at C286 in the transmembrane domain (Figure 1), and C286A mutation blocks antibody-induced HA binding.[182] PMA-induced (phorbol 12-myristate 13-acetate) HA binding is also associated with the formation of disulfide bonds via C286.[183] CD44 dimers artificially formed by creating CD44:CD3ζ chimeras with the transmembrane domain of CD3ζ promotes CD44-HA binding.[184] Other reports show that CD44 dimers and clusters normally exist in cells. For example, bioluminescent resonance energy transfer (BRET) experiments detect dimer formation of CD44 in HEK 293 R cells transfected with full-length CD44.[185] Disulfide-linked CD44 homodimers are also observed in unstimulated or TPA-stimulated CD44-transfected NIH3T3 Swiss mouse embryonic fibroblasts.[186] Those dimers appear to have additional stabilization arising from interactions between the ECD domains, and excess soluble CD44 ECD can disrupt the dimers. Collectively, these studies predict that CD44 clustering or at least dimerizing is a requirement for efficient binding of HA to intact cells.

Further, nanoscale clustering of CD44 dimers contributes to increasingly high-affinity HA binding. Quantitatively, stable CD44 binding to HA requires a "threshold" surface density of CD44, whether on cells, or as an isolated protein coupled to beads. The absolute value of a required threshold density for binding is modulated by N-glycosylation, where greater N-glycosylation reduces affinity and increases the threshold value required for binding.[163] A theoretical model explaining this phenomenon is provided by Dubacheva, Richter, and coworkers.[187] Using the experimental data of English et al.[163] and a model for multivalent probes (like HA) binding to surfaces bearing multiple target molecules (like CD44), HA affinity for CD44 was predicted to depend on the CD44 surface density to the 4th power. This results in such a strong density dependence that low density yields apparently undetectable HA binding, but a rapid increase in binding is observed as the density increases, resembling a "threshold density" requirement. Above the "threshold," every two-fold increase in density is predicted to result in a 16-fold increase in HA binding. When the additional differences in monomeric CD44 affinity for HA resulting from N-glycosylation are considered, this model accounts for the apparent absence of HA binding by cells lacking sufficient affinity and surface presentation density.[187]

Isolated recombinant CD44 fragments duplicate these in vivo binding properties. Although monomeric CD44 ECD binds HA in solution, an ECD dimer created by expression of the HABD in fusion with IgG Fc (CD44-Fc) has a stronger affinity.[188] Surface display can also have the effect of creating arrays that mimic in vivo CD44 dimer properties. For example, Richter and coworkers showed that immobilizing tailless monomeric His-tagged CD44 HABD on a supported Ni-NTA lipid bilayer allows it to acquire the equivalent HA binding properties of a CD44 dimer in vivo including molecular weight dependence of binding affinity. Larger HA polymers bind to surface-attached CD44 irreversibly, while short HA (<10 kDa) binds reversibly.[189] Peer and coworkers also showed that immobilized CD44-Fc exhibits molecular weight-dependent HA binding using SPR.[190]

It is interesting to note that, while CD44 clustering affects HA binding affinity, CD44 clustering is also induced or modulated by HA, in a manner dependent upon its molecular weight. "Capping" of CD44 on the cell surface is induced by HA binding.[191] A FRET study also showed that HMW HA-CD44 interactions cluster CD44, while HA oligosaccharides do not. Rather, HA oligosaccharides reduce the

clustering caused by HMW HA.[192] HMW HA-induced clustering of CD44 is enhanced by chemical crosslinking of HA[192] and by TSG-6 catalysis of HA crosslinking via HC modification.[193]

An interplay between receptor clustering and HA crosslinking has also been observed for the LYVE-1 HA receptor, which has a similar sequence and domain structure to CD44. Jackson and coworkers have shown that LYVE-1 requires a critical threshold density on the cell surface for HA binding, and an antibody that crosslinks LYVE-1 results in strong HA binding. Microscopy shows the receptors are nano-clustered. As is observed for CD44, LYVE-1 shows enhanced affinity for HA crosslinked by full-length TSG-6.[194] LYVE-1 differs from CD44 in that its binding to HA requires a minimum of a dimer of the receptor, with monomers linked by a disulfide bridge in the membrane proximal domain.[195] For either CD44 or LYVE-1, high MW is important for HA binding because it enhances receptor clustering and the consequent downstream signaling.[170]

HA binding affinity and patterning depend on CD44-cytoskelton interactions (and vice versa)

The CD44 ICD binds to actin through interactions with ezrin, radixin, moesin (ERM) and ankyrin, and binding affinities are dependent on the phosphorylation status of both CD44 and the partner proteins.[18,196–198] This linkage of CD44 to the actin cytoskeleton leads to an organizational motif or patterning of CD44 on the cell surface. For example, a repetitive pattern of CD44 patches, spaced about 41–45 nm on human chondrosarcoma and bladder carcinoma cells, as well as on bovine articular chondrocytes, is detected by anti-CD44 antibodies. A similar repetitive pattern, detected using anti-KS antibodies, occurs in pericellular matrices of aggrecan and HA, with a slightly longer repetitive spacing of 60–70 nm.[199]

A compelling model for organization of the cell membrane into compartments that are separated by fence-like barriers has been proposed in which transmembrane CD44 molecules serve as pickets connecting the intracellular actin cytoskeleton and an extracellular HA/proteoglycan pericellular matrix. Single-molecule localization and diffusion measurements of CD44 showed that approximately 20% of macrophage CD44 is immobile, 30% is mobile and 50% is alternately confined or mobile. CD44 mobility is affected by the integrity of the actin cytoskeleton, so that crosslinking actin reduces CD44 mobility, while disrupting actin liberates CD44 to move freely in the plasma membrane. In this model, HA functions as an exoskeleton to organize the picket fence. Thus, HA and CD44 reciprocally reduce each other's mobility and control lateral diffusion and dimerization of other cell surface receptors.[4,200,201]

Further support for the picket fence model has been obtained using CD44 constructs of varying truncations of the core protein, with dye-SNAP (19 kDa) linked to its N-terminus and GFP (27 kDa) to its C-terminus, to detect spatial/temporal localization of CD44 by high-resolution imaging. Results show a meshwork of CD44 and identify the ICD sequence as the major determinant for CD44 confinement. This mobility restriction depends on the dynamics and remodeling of formin-nucleated F-actin filaments. However, CD44 nanoscale clustering within/along the meshwork depends on both the ICD and ECD, due to the additional modulation of clustering by HA binding.[202]

It is interesting to contrast the two HA receptors CD44 and LYVE-1 with respect to relationship with the actin cytoskeleton. LYVE-1 does not coimmunoprecipitate with actin or ezrin, and is not colocalized along the actin filament network, but is instead corralled within the compartments created by the actin meshwork, with reduced diffusion across barriers and consequent reduced dimerization or clustering. Disruption of the actin network increases LYVE-1 clustering and HA binding affinity.[203]

Lipid raft localization of CD44 and its effect on HA binding

CD44 binding to HA may also be affected by reversible localization of CD44 in plasma membrane microdomains referred to as lipid rafts. Lipid raft domains are characterized by a high content of tightly packed sphingolipids and cholesterol, resistance to solubilization by detergents, restricted lateral mobility of embedded proteins, and colocalization of multiple transmembrane receptor proteins, that collectively create a signaling platform. The fraction of CD44 found in lipid rafts is highly dependent on cell type and context.[204] For example, only about 10% of CD44 in human dermal fibroblasts is localized in lipid rafts, whereas about 40% of CD44 is in rafts in myofibroblasts.[205] In breast cancer cells, migration is coupled with a change in CD44 localization from primarily inside lipid rafts to outside these domains.[206] Because lipid raft integrity depends on cholesterol, depletion of cholesterol using methyl-β-cyclodextrin, or by reduction of cholesterol levels with statins, releases CD44 from raft domains, and results in dispersal throughout the plasma membrane.[207–209]

Multiple covalent modifications of CD44 can reversibly alter its localization within lipid rafts. The primary driver of lipid raft localization is enzymatically catalyzed S-acylation with palmitic acid on C286 in the TM domain and C295 in the membrane-proximal ICD.[156,157,206,210,211] The reversible addition of sialic acid to oligosaccharides on the extracellular domain of CD44 also drives partition into lipid rafts, and controls CD44 functional co-localization with EGFR.[212,213] Phosphorylation of S325 in the ICD of CD44 is associated with lipid raft localization, and de-phosphorylation causes CD44 to move out, homodimerize, and interact with ezrin.[198]

HA can be bound by CD44 inside or outside lipid rafts.[156,198,204,205] Outside lipid rafts, CD44 homodimerization, and clustering, binding to the actin cytoskeleton via ERM proteins, and a reduction in sialylation favor HA binding. Indeed, HA binding has been reported to increase in primary T lymphocytes after disruption of rafts by cholesterol removal.[208] HA binding to CD44 within lipid rafts is increased by the association of this receptor with ankyrin.[210,214,215] HA:CD44 binding is required for functional heterodimeric complexes with EGFR[205,216,217] and requires covalent

modification of HA by TSG-6-catalyzed heavy chain 5 (HC5) transfer from inter-α-inhibitor.[218] HC5-modified HA, complexed with CD44-EGFR in lipid rafts, supports fibroblast-to-myofibroblast differentiation.[218]

HA in CD44 proteolytic cleavage and shedding

CD44 that is localized in lipid rafts as a result of palmitoylation of C286 in the TM domain can undergo turnover by endocytosis, with bound HA.[156] In contrast, CD44 located outside lipid rafts is susceptible to cleavage in the stem region near the membrane surface by metalloproteinases (Figure 1), for example, MT1-MMP, ADAM10, ADAM17, and MMP9, resulting in shedding of the ECD (and its attached HA) into the microenvironment.[219] Subsequent cleavage of CD44 within the TM domain by presenilin-1 in the γ-secretase complex releases the ICD and a short hydrophobic peptide, CD44β, into the cytoplasm.[220,221] The free CD44 ICD translocates to the nucleus, and is implicated in transcriptional activation of multiple genes,[222] notably MMP9. Cleavage of the CD44 ectodomain promotes the motility of fibroblasts and keratinocytes, and inhibition of cleavage reduces cell migration on an HA-coated surface.[223]

Cleavage by MT1-MMP has been reported to be most active in invasive cancer cells, whereas cleavage by an ADAM protease occurs in both normal and tumor tissues. MT1-MMP associates with CD44 through interaction of the cytoplasmic tails of each protein with an ERM protein. A detailed structural analysis of the interaction of radixin with MT1-MMP and CD44 has been provided by Hakoshima and coworkers.[224] This complex places the extracellular hemopexin-like domain of MT1-MMP in position for complexation with CD44,[225,226] and facilitates access of the protease catalytic domain for CD44 cleavage, at CD44 G192 or G233 (less frequent).[227,228]

The alternative cleavage by an ADAM protease occurs at S249.[228] The ADAM proteases are differentially regulated.[229,230] ADAM10 is activated by influx of extracellular Ca^{2+}, including that caused by stretch-activated channels during cell migration, which regulates calmodulin association with the enzyme. ADAM17 is activated by phorbol ester stimulation, via activation of PKC and small GTPase Rac1. Disulfide-linked CD44 dimers and CD44-protease heterodimers play a role in binding to, and cleavage by, ADAM10 in CD44-transfected NIH3T3 Swiss mouse embryonic fibroblasts.[186]

Because HA binding to CD44 is known to cause partial unfolding and/or increased flexibility of the C-terminal extension from the CD44 Link module, HA could increase susceptibility of CD44 to proteolytic cleavage by increasing accessibility of cleavage sites. HMW HA, however, can create steric hindrance to protease access, either directly by excluded volume or indirectly by multimolecular clustering CD44. In contrast, the binding of short HA fragments to CD44 likely facilitate CD44 proteolysis and shedding, modulating cellular response to HA.[166,222,223,227] In evidence for this concept, HA fragments containing 6–36 monosaccharides, but not shorter oligomers and not HA polymers of 36–1000 kDa, increase proteolytic cleavage and shedding of the CD44 ectodomain in pancreatic carcinoma cells.[231,232]

BACKGROUND OF EXTRACELLULAR, CELL SURFACE RHAMM

RHAMM was discovered as an extracellular HA-binding protein that was isolated from the spent culture medium of sparse, actively motile, embryonic fibroblasts, and shown to be required for motility of these cells.[233] RHAMM is now known to function in multiple subcellular compartments. As example, RHAMM impacts the organization of microtubules, centrosomes, and the mitotic spindle,[11] is rapidly and transiently increased during G2M of the cell cycle, and is required for transition through G2M.[11,234,235] RHAMM is present in cell nuclei, where it participates in transcriptional complexes such as E2F1.[236] Excellent reviews have described these intracellular RHAMM functions that may or may not be associated with its extracellular HA binding activity.[13,21,237,238] This review focuses upon the known mechanisms that underlie the signaling functions of RHAMM as an extracellular HA binding and CD44-associated protein.

The presence of RHAMM on the cell surface became controversial because it does not contain a signal peptide for export through the Golgi/ER or a membrane-spanning sequence needed to initiate signaling, and is clearly present in intracellular compartments.[239–241] Currently, the manner in which RHAMM is both exported and able to activate motogenic signaling cascades from an extracellular space is incompletely understood.[11,15] However, RHAMM is one of many cytoplasmic proteins that are exported by unconventional or unknown mechanisms during tissue injury and cellular stress.[12,242] Evidence suggests that cell surface RHAMM activates signaling cascades by an association with integral receptors including CD44 and growth factor receptors.[3,13,15] These collective results predict that extracellular RHAMM functions as a coreceptor.

Compelling evidence that RHAMM isoforms are transferred to the cell surface has accrued from conventional biochemical analyses using RHAMM-specific antibodies. Thus, immuno-reactive RHAMM proteins are detected with live cell surface labeling[243,244] and on isolated plasma membranes (e.g, Figure 2A,B). Extracellular RHAMM has also been visualized with both scanning (Figure 2C) and transmission (Figure 2D) electron microscopy, and by flow cytometry.[8,15,245] Furthermore, anti-ZSGP antibodies detect transfected ZSGP-tagged RHAMM in nonpermeabilized fibroblasts (Figure 2E and Messam et al.[15]). However, the most compelling evidence for extracellular RHAMM derives from many reported functional assays. Thus, both blocking anti-RHAMM antibodies[5,6,244,246–250] and RHAMM peptide mimetics[35,247,250–253] inhibit the motility of a variety of cell types. Add-back experiments show that the motility defects of *Rhamm*-deficient fibroblasts are rescued by the addition of purified recombinant RHAMM protein linked to Sepharose beads to prevent its internalization.[5] Cell-surface RHAMM-regulated migration is particularly important for normal tissue repair and is required

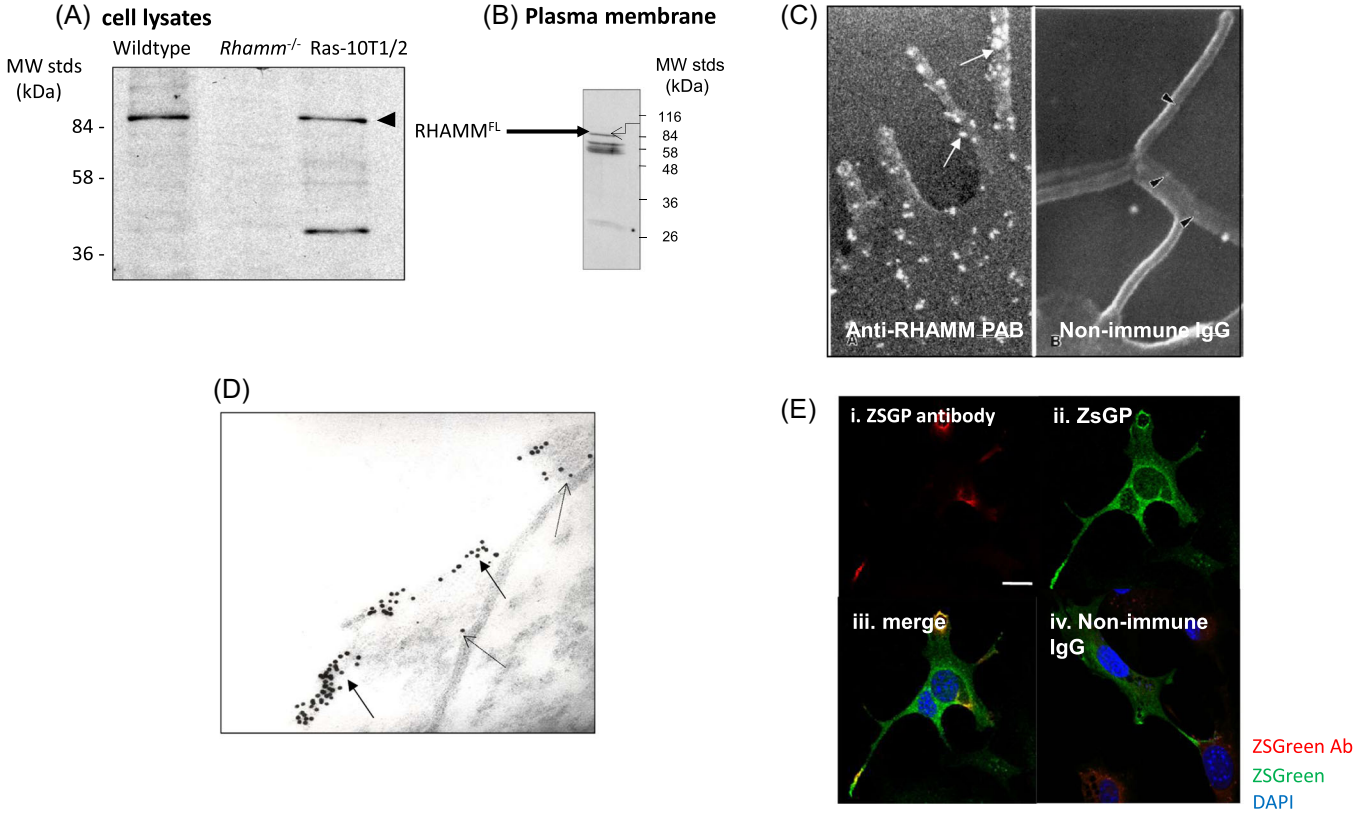

FIGURE 2 Cell surface display of RHAMM on fibroblasts. Western blots of RHAMM in cell lysates (A) and isolated plasma membranes (B). RHAMM is expressed as a 95 kDa full-length protein in wildtype mouse fibroblasts, and is not detected in *Rhamm*-null counterparts. Western blots of RHAMM expression in plasma membranes purified from Ras-10T1/2 fibroblasts show presence of full-length and shorter RHAMM isoforms. (C) Scanning and (D) transmission electron microscope images of gold-RHAMM antibody beads decorating the cell surface of fibroblasts. Nonimmune IgG serves as a control. (E) *Rhamm*$^{-/-}$ fixed, nonpermeabilized fibroblasts rescued with a Zoanthus sp. green fluorescent protein (ZSGP)-tagged *Rhamm* complementary DNA (cDNA), and stained with a ZSGP antibody, which detects exported, cell surface ZSGP-RHAMM in cell processes (i). ZSGP fluorescence is also detected in the cytoplasm and nucleus (ii), and is not detected by the ZSGP antibody confirming the cell surface location of antibody staining in (i). The merge image (iii) and nonimmune IgG (iv) serve as controls confirming the antibody specificity for ZSGP. IgG, immunoglobulin G; RHAMM, receptor for hyaluronan-mediated mobility.

for innate immune cell influx to initiate inflammation,[8,254] migration of both smooth muscle and endothelial cells to promote neo-angiogenesis,[245,248,250] and migration of leader mesenchymal cells to initiate dermal repair.[7,243] Deregulation of the fundamental function of RHAMM in promoting the migration of these cell types contributes to disparate disease processes including vascular disease[238] and cancer progression. For example, cell surface RHAMM mediates migration of breast cancer cells toward and into vascular networks.[3,6,237]

One RHAMM ligand that appears to be required for its motogenic signaling activation is HA. For example, the induction of Ras-transformed fibroblast motility, which display extracellular RHAMM, is blocked by hyaluronidase digestion, the HA-binding region of aggrecan used as a competitor for HA binding to cellular receptors, and blocking anti-RHAMM antibodies. HA rescues the motility of hyaluronidase-treated cells but not in the presence of RHAMM antibodies.[249] It is notable that RHAMM does not always function to promote celll motility[7,255,256] and this may result from its intracellular sequestration and/or its association with partner proteins such as CD44. Here, we review the biology of extracellular RHAMM from the perspective of its extracellular association with HA and CD44.

Rhamm gene and protein structure

A *Rhamm* complementary DNA (cDNA) was first isolated by screening an expression library constructed from Ras-transformed murine 3T3 cells using a monoclonal antibody prepared against purified RHAMM protein.[257] Start and stop codon analyses predicted the encoded amino acid sequence to have a molecular weight of 52.2 or 46.7 kDa.[240] Later studies showed that the full-length mouse RHAMM gene is longer, contains multiple stop codons, and encodes a 95 kDa protein transcribed from 18 exons.[241] The human *RHAMM* gene encodes a slightly shorter protein of 84 kDa[239]: the mouse *Rhamm* gene is longer due to a repeated sequence in exon 12.[241,258] Transcription of *RHAMM* is subject to alternative splicing and this, as well as potential alternative start codon usage, generates multiple protein variants. Although the

functions of RHAMM isoforms are understudied these can be differentially expressed, and evidence indicates they exhibit distinct oncogenic properties. For example, a shorter than full-length RHAMM protein is expressed after tissue injury,[250] and is transforming in fibroblasts[259] while variant forms of human RHAMM exhibit different oncogenic potential in mouse models of pancreatic cancer.[260] More detailed descriptions of RHAMM variant forms and their functions have been described.[15,261,262]

Based on the cDNA sequence, the predicted RHAMM protein sequence is predominately hydrophilic, rich in glutamic acid, lysine, and glutamine but also leucine.[240,257] As noted above, RHAMM resembles a cytoplasmic protein in its absence of a known export motif, membrane spanning domain, and does not carry a GPI anchor. The conformation of human RHAMM has been predicted to be almost entirely alpha-helical by the AlphaFold AI system (https://alphafold.ebi.ac.uk/entry/O75330) (Deep Mind and EMBL-EBI)[263,264] (Figure 3). It has also previously been predicted to assemble into a coiled-coil structure,[265] based on the appearance of three leucine residues spaced seven amino acids apart near the C terminus, as in the leucine zipper motif, but the solution conformation has not yet been experimentally determined. This motif may play a more important role in intracellular RHAMM interactions with transcription factors and other signaling proteins.

RHAMM binds to HA

RHAMM and its variant forms have been isolated by retention on affinity matrices of HA covalently attached to Dowex resin or to Sepharose.[35,233,266] These RHAMM proteins also bind radiolabeled or biotinylated HA[267,268] in far western assays and to HA in solution using isothermal calorimetry. Reciprocally, HA deposited on nitrocellulose membranes binds to radiolabeled RHAMM, with an apparent K_D for HA binding of approximately 10 nM.[267] The ability of RHAMM to bind to HA has been confirmed by multiple independent groups, and inferred by evidence that a response to HA requires RHAMM expression.[269–273]

The location of the HA binding site to the C-terminus on mouse RHAMM was first established by increasing truncations of recombinant proteins,[274] then the aa required for binding to HA were identified by site-directed mutagenesis of positively charged aa. These analyses identified two domains with clustered basic amino acids in a BX_7B motif that contained HA-binding activity (residues 635–643 and 657–665 in Figure 3). Mutation of either of these two positively charged sequences reduces the RHAMM binding affinity for HA, suggesting that both participate in binding HA. These studies also predict that the RHAMM-HA interaction is predominately electrostatic, consistent with evidence that binding is disrupted with 1 M NaCl. Considering the RHAMM segment from residues 635–671, which in the human RHAMM sequence includes both BX_7B sequences, there are 12 K + R, 1 H, and 4 D + E, for a net positive charge of 8 or 9, depending on the protonation of histidine. Figure 3 also portrays HA8, with four negatively charged carboxyl groups, in a left-handed helical structure determined by X-ray fiber diffraction (Figure 3). The HA8 structure was placed (not computationally docked or energetically minimized) adjacent to the AlphaFold predicted structure for the RHAMM HABD, for illustration of relative dimensions and potential electrostatic interactions.

An alternative structure for the HA-binding region of RHAMM was later proposed based on NMR analysis of a 60-residue model for murine RHAMM commencing 14 amino acids upstream of K635 (here we have altered the numbering used in that paper to coincide with the human segment numbering shown in Figure 3), and containing both putative HA-binding sites.[275] The proposed structure is predominantly alpha-helical, but broken into three segments joined by two short loops allowing the helical sections to fold back into a

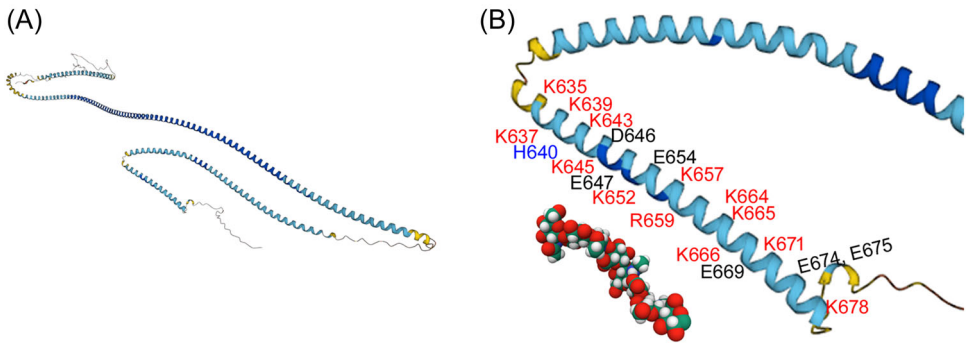

FIGURE 3 RHAMM and its HA binding site. (A) Human RHAMM conformation is predicted to be mainly alpha-helical. The N terminal is near the top of the image, and the C terminal is near the bottom. Downloaded from https://alphafold.ebi.ac.uk/entry/O75330 (Deep Mind and EMBL-EBI). (B) The HA binding region of human RHAMM reveals a high density of basic amino acid residues, located in two BX_7B clusters (aa 635–643 and 657–665) separated by a short segment containing several acidic residues. The full length of the protein segment from aa 635–671 carries a net positive charge of 8–9. For visual size comparison only, an octasaccharide of HA (HA8) carrying four carboxyl groups is placed adjacent to the RHAMM segment. The HA8 structure image was from the RCSB PDB (rcsb.org), PDB ID 3HYA (https://doi.org/10.2210/pdb3HYA/pdb), (Guss et al.[50]), visualized with Mol* software (D. Sehnal, S. Bittrich, M. Deshpande, R. Svobodová, K. Berka, V. Bazgier, S. Velankar, S. K. Burley, J. Koča, A. S. Rose. *Nucleic Acids Res.* **2021**. https://doi.org/10.1093/nar/gkab314).

bundle. One break in the alpha helix is proposed to occur at the end of the first BX_7B site, followed by a 5-residue loop and a second helical segment extending to the end of the second BX_7B site. An additional 2-residue loop allows a third helix to fold and join the helical bundle. This proposed RHAMM structure computationally docks with a dodecasaccharide of HA. The HA chain adopts a kinked conformation, allowing formation of three salt bridges from HA glucuronate carboxyl groups to K652, K657, and K664. Interestingly, K652 is located between the two BX_7B domains, and was not considered to be part of the critical HA-binding sequence in the previous mutational studies. Further studies are warranted to reconcile these discrepancies but both of these models predict that the mechanism by which HA binds to RHAMM is significantly different from CD44-HA interactions.

CONCEPTS AND CONCLUSIONS

Since RHAMM is a peripheral extracellular HA-binding protein, it's signaling functions must result from an association with integral membrane proteins. Identified proteins that RHAMM physically and/or functionally associates with include CD44, TLRs, and growth factor receptors including EGFR, PDGFR, TGFBR1, and RON.[3,237] RHAMM is normally absent or expressed at low levels in homeostatic conditions, but is transiently increased during tissue stress and response to injury such as cutaneous wounding, and is constitutively expressed in most cancers[15,276,277] and inflammation-based diseases. This pattern of expression is in contrast to that of CD44, which is generally constitutively expressed during tissue homeostasis. Considering the affinity of RHAMM for HA, and the tethering of HA to CD44 at the cell surface, it is important to understand the interplay of these three macromolecules. RHAMM, particularly extracellular RHAMM, appears to be transiently expressed, senses HA polymer density[278] and modifies CD44 signaling to mediate a stress response. The association of extracellular RHAMM with CD44, which is considered here, is based upon studies showing that they can physically interact and alter each other's spatial (extracellular) distribution. Additionally, their expression is often coregulated and they display some overlapping and mutually dependent functions.

Evidence for a physical association of CD44 and RHAMM is provided by their colocalization, particularly in the cell processes of actively motile cells, demonstrated by confocal immunofluorescence and FRET.[279] The extent of extracellular colocalization is affected by how their mutual ligand, HA, is presented. Thus, HA in solution has little effect on the association of CD44 with RHAMM although tethering HA to the substratum as occurs in vivo increases their association detected by FRET. The expression and colocalization of these two receptors also depend upon the concentration of HA encountered by cells with RHAMM expression being more sensitive to HA concentration gradients predicting that extracellular RHAMM is a sensor of increasing concentrations of HA.[278]

An association of RHAMM with CD44 has also been demonstrated by coimmunoprecipitation in migrating fibroblasts, sarcomas, and the highly motile triple-negative breast cancer cell line, MDA-MB-231 cells. This association is not detected in the less motile MCF7 breast cancer and other cell lines. The RHAMM/CD44 complexes formed in fibroblasts and MDA-MB-231 cells function to activate intracellular signaling such as the ERK1,2 pathways required for cell motility.[280] Although these reports identify cell and culture conditions that result in an association of CD44 with RHAMM, they do not indicate the nature of this interaction. Thus, to our knowledge, it has not yet been reported if an association between RHAMM and CD44 results from a direct protein:protein interaction or is indirect, for example, bridged by HA. Regardless of how they associate with one another, RHAMM and CD44 exhibit overlapping as well as distinct functions that strongly impact cell motility. A number of independent reports show that extracellular RHAMM and CD44 are both required for maintaining motility velocity, demonstrated by a similar and nonadditive effect of blocking anti-CD44 and RHAMM antibodies on this motility characteristic. Further, the effect of RHAMM/CD44 complexes result from activation of a number of signaling pathways including ERK1,2/MEK. However, the two proteins can have distinct motogenic functions. For example, studies show that RHAMM uniquely regulates the directionality of breast cancer cells migrating toward endothelial cells. Distinct functions and cell-context-dependent formation of CD44/RHAMM complexes involved in cell motility may be due to differences in regulation of their expression and/or mutual effects of these two proteins on each other's extracellular display.[6]

RHAMM and CD44 are often coexpressed during processes such as wounding, neovascularization,[238] inflammation, cancer, and inflammation-based diseases.[3,13] Using cancer as a disease example, even when RHAMM expression is elevated, however, this relationship is clearly complex. Thus, probing TCGA PanCancer Atlas reveals that the expression of these two HA-binding proteins can be inversely, positively, or not correlated depending on the cancer type (Table 1). For example, CD44 and RHAMM expression is positively correlated in bladder, colorectal, cervical, and kidney cancers but inversely correlated in prostate and breast cancers, and not correlated in head and neck cancers. This complex relationship does not appear to affect the association of either protein with disease outcome parameters, which may be due, in part, to overlapping, redundant functions.

Several studies predict that both RHAMM and CD44 influence each other's spatial distribution, which of course also impact their ability to form complexes. As examples, forced expression of CD44v7 results in internalization of extracellular RHAMM in endothelial cells.[6] Conversely, cell surface RHAMM forms complexes with and promotes clustering of CD44s into the processes of migrating skin fibroblasts that are responding to wounding.[5] Thus, extracellular RHAMM-coupled beads rescue the motility deficiency of *Rhamm*$^{-/-}$ skin fibroblasts in a CD44-dependent manner, and promote CD44 display/clustering in cell processes. In contrast to skin fibroblasts, loss of either CD44 or RHAMM promotes rather than reduces the motility of keratinocytes in a setting of wounding.[7] In this context, the

promoting effect of *Rhamm*-loss on keratinocyte motility was traced to stimulation of MMP9 expression and a consequent MMP-dependent CD44 shedding. Although RHAMM also regulates MMP9 expression in skin fibroblasts, *Rhamm*-loss reduces rather than promotes MMP9 expression. Intriguingly, migration of skin fibroblasts, responding to a wounding stimulus, requires MMP9, the mechanism of action does not appear to involve promoting CD44 shedding but appears to involve clustering and subsequent internalization of CD44[5] (Figure 4). This opposing effect of RHAMM and MMP9 on CD44 shedding and motility in skin fibroblasts versus keratinocytes may be related to differential expression levels or variant forms of CD44 and susceptibility of CD44 to proteases or to differences in the contribution of CD44 to the motility of cells that exist as groups (keratinocytes) versus in isolation (fibroblasts). Nevertheless, these collective results show that RHAMM and CD44 influence each other's cell surface display and spatial organization at the plasma membrane. This ability is predicted to also modify the spatial organization of other binding partners particularly in the setting of a wound stimulus.

TABLE 1 Coexpression of RHAMM/HMMR and CD44 mRNA in cancers.

Cancer type	Correlation coefficient	*p* Value
Bladder	+0.156	1.75e−3
Colorectal	+0.186	1.69e−5
Breast	−0.146	3.88e−6
Cervix	+0.178	3.13e−3
Cutaneous melanoma	−0.105	0.046
Kidney (clear cell)	+0.338	7.62e−11
Acute myeloid leukemia	−0.286	2.42e−4
Pancreas	−0.311	4.03e−5
Pediatric neuroblastoma	−0.293	4.23e−4
Prostate	−0.188	2.85e−5
Testes	−0.343	2.50e−5
Uveal melanoma	−0.252	0.024

Note: The coexpression of RHAMM and CD44 TCGA Pan-Cancer Atlas databanks available on cBioportal Cancer Genomics (http://www.cbioportal.org). RHAMM and CD44 were not coexpressed in a number of other cancers including Adrenal, Glioblastoma multiforme, head and neck, and liver. Spearman coefficients are presented.

Abbreviation: HMMR, hyaluronan-mediated motility receptor; mRNA, messenger RNA; RHAMM, receptor for hyaluronan-mediated mobility.

In summary, studies clearly show that the association of extracellular RHAMM with CD44 has important consequences to cellular functions that are relevant to many diseases including aberrant inflammation and cancer progression. CD44 is a particularly attractive therapeutic target in cancer since it is a marker for cancer-initiating cells and the HA-binding properties of CD44 are considered to be key to metastatic progression, which is currently a barrier to effective management of many cancers. However, targeting CD44 has proven to be toxic likely because it is multifunctional and constitutively expressed in most normal tissues. CD44 clustering, attachment to the actin cytoskeleton via ERM/ankyrin/merlin, and attachment to pericellular HA create the platform upon which at least some of the functions of other HA binding proteins and receptors depend including RHAMM. RHAMM is a promising alternative target to CD44 since it is poorly or not expressed under homeostatic

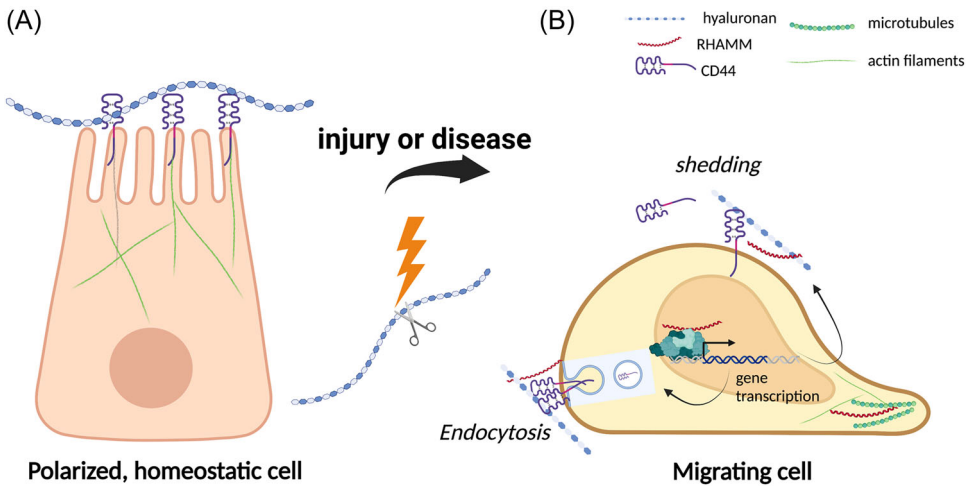

FIGURE 4 Model for RHAMM-regulation of CD44 spatial organization. (A) In normal homeostatic cells, CD44 creates discreet well-organized membrane domains that are corralled by its binding to high molecular weight HA. Domains are held in place by linkage of CD44 ICD with the actin cytoskeleton. (B) Injury, cell stress, or disease (e.g., cancer) results in HA fragmentation and expression as well as extracellular export of RHAMM isoforms, which disrupt the symmetry of CD44-mediated domain structure. Extracellular RHAMM binds to HA fragments and associates with CD44 to activate signaling pathways that ultimately result in either CD44 shedding or its endocytosis/internalization depending upon the cell type. Intracellular RHAMM and the released ICD of CD44 participate in transcriptional complexes that regulate gene expression required for cell migration. Intracellular RHAMM also associates with cytoskeleton elements required for cell motility. Model created with Biorender.com. HA, hyaluronan; ICD, intracytoplasmic domain; RHAMM, receptor for hyaluronan-mediated mobility.

conditions and is required for CD44-mediated processes (e.g., cell motility) that are relevant to cancer metastasis and to other diseases that are contributed to by aberrant motility such as chronic inflammation.

Although the associations and functional consequences of RHAMM:CD44 interactions with HA are only beginning to be probed and revealed, they offer promise of novel therapeutic intervention tools to manage the many intractable diseases that result from aberrant motility, which include cancer metastasis, and heightened inflammatory responses leading to tissue fibrosis.

AUTHOR CONTRIBUTIONS

Mary K. Cowman: Conceptualization; formal analysis; methodology; project administration; visualization; writing—original draft; writing—review and editing. **Eva A. Turley**: Conceptualization; data curation; formal analysis; funding acquisition; investigation; methodology; project administration; resources; visualization; writing—original draft; writing—review and editing.

ACKNOWLEDGMENTS

Work was supported by the Cancer Research Society (ET) and Internal Research Funding (Lawson Health Research Institute) (ET).

CONFLICT OF INTEREST STATEMENT

The authors declare no conflict of interest.

DATA AVAILABILITY STATEMENT

Data available on request from the authors.

ETHICS STATEMENT

The authors have nothing to report.

ORCID

Mary K. Cowman http://orcid.org/0000-0003-2714-1666
Eva A. Turley http://orcid.org/0000-0002-7383-4896

REFERENCES

[1] G. L. Nicolson, G. Ferreira de Mattos, *Biochim. Biophys. Acta Biomembr*. **2023**, *1865*(4), 184135.
[2] A. Erazo-Oliveras, M. Munoz-Vega, M. L. Salinas, X. Wang, R. S. Chapkin, *FEBS J*. **2022**. https://doi.org/10.1111/febs.16665
[3] C. Tolg, B. J. A. Messam, J. B. McCarthy, A. C. Nelson, E. A. Turley, *Biomolecules* **2021**, *11*(11), 1551.
[4] S. M. Mylvaganam, S. Grinstein, S. A. Freeman, *Semin. Immunopathol*. **2018**, *40*(6), 605.
[5] C. Tolg, S. R. Hamilton, K. A. Nakrieko, F. Kooshesh, P. Walton, J. B. McCarthy, M. J. Bissell, E. A. Turley, *J. Cell Biol*. **2006**, *175*(6), 1017.
[6] D. J. Wessels, C. Pujol, N. Pradhan, D. F. Lusche, L. Gonzalez, S. E. Kelly, E. M. Martin, E. R. Voss, Y. N. Park, M. Dailey, S. L. Sugg, S. Phadke, A. Bashir, D. R. Soll, *Cell Adh. Migr*. **2021**, *15*(1), 224.
[7] C. Tolg, M. Liu, K. Cousteils, P. Telmer, K. Alam, J. Ma, L. Mendina, J. B. McCarthy, V. L. Morris, E. A. Turley, *J. Biol. Chem*. **2020**, *295*(16), 5427.
[8] S. Garantziotis, R. C. Savani, *Matrix Biol*. **2019**, *78–79*, 1.
[9] R. Stern, A. A. Asari, K. N. Sugahara, *Eur. J. Cell Biol*. **2006**, *85*(8), 699.
[10] S. M. Ruppert, T. R. Hawn, A. Arrigoni, T. N. Wight, P. L. Bollyky, *Immunol. Res*. **2014**, *58*(2-3), 186.
[11] C. A. Maxwell, J. McCarthy, E. Turley, *J. Cell Sci*. **2008**, *121*(Pt 7), 925.
[12] D. C. Radisky, M. Stallings-Mann, Y. Hirai, M. J. Bissell, *Nat. Rev. Mol. Cell Biol*. **2009**, *10*(3), 228.
[13] A. M. Carvalho, R. L. Reis, I. Pashkuleva, *Adv. Healthcare Mater*. **2023**, *12*(5), e2202118.
[14] L. Schaefer, *J. Biol. Chem*. **2014**, *289*(51), 35237.
[15] B. J. Messam, C. Tolg, J. B. McCarthy, A. C. Nelson, E. A. Turley, *Int. J. Mol. Sci*. **2021**, *22*(19), 10313.
[16] J. Lesley, R. Hyman, N. English, J. B. Catterall, G. A. Turner, *Glycoconjugate J*. **1997**, *14*(5), 611.
[17] D. Naor, S. Nedvetzki, M. Walmsley, A. Yayon, E. A. Turley, I. Golan, D. Caspi, L. E. Sebban, Y. Zick, T. Garin, D. Karussis, N. Assayag-Asherie, I. Raz, L. Weiss, S. Slavin, I. Golan, *Ann. N. Y. Acad. Sci*. **2007**, *1110*, 233.
[18] H. Ponta, L. Sherman, P. A. Herrlich, *Nat. Rev. Mol. Cell Biol*. **2003**, *4*(1), 33.
[19] V. Orian-Rousseau, J. Sleeman, *Adv. Cancer Res*. **2014**, *123*, 231.
[20] P. Heldin, C. Kolliopoulos, C. Y. Lin, C. H. Heldin, *Cell Signal*. **2020**, *65*, 109427.
[21] M. A. Pibuel, D. Poodts, M. Díaz, S. E. Hajos, S. L. Lompardía, *J. Biol. Chem*. **2021**, *296*, 100549.
[22] A. G. Tavianatou, I. Caon, M. Franchi, Z. Piperigkou, D. Galesso, N. K. Karamanos, *FEBS J*. **2019**, *286*(15), 2883.
[23] B. Weissmann, K. Meyer, P. Sampson, A. Linker, *J. Biol. Chem*. **1954**, *208*(1), 417.
[24] K. Meyer, *Fed. Proc*. **1958**, *17*(4), 1075.
[25] N. Itano, T. Sawai, M. Yoshida, P. Lenas, Y. Yamada, M. Imagawa, T. Shinomura, M. Hamaguchi, Y. Yoshida, Y. Ohnuki, S. Miyauchi, A. P. Spicer, J. A. McDonald, K. Kimata, *J. Biol. Chem*. **1999**, *274*(35), 25085.
[26] N. Itano, K. Kimata, *IUBMB Life* **2002**, *54*(4), 195.
[27] P. H. Weigel, V. C. Hascall, M. Tammi, *J. Biol. Chem*. **1997**, *272*(22), 13997.
[28] M. K. Cowman, H. G. Lee, K. L. Schwertfeger, J. B. McCarthy, E. A. Turley, *Front. Immunol*. **2015**, *6*, 261.
[29] L. B. Dahl, I. M. Dahl, A. Engstrom-Laurent, K. Granath, *Ann. Rheum. Dis*. **1985**, *44*(12), 817.
[30] H. G. Lee, M. K. Cowman, *Anal. Biochem*. **1994**, *219*(2), 278.
[31] U. B. G. Laurent, K. A. Granath, *Exp. Eye Res*. **1983**, *36*(4), 481.
[32] M. W. Holmes, M. T. Bayliss, H. Muir, *Biochem. J*. **1988**, *250*(2), 435.
[33] R. Tammi, U. M. Ågren, A. L. Tuhkanen, M. Tammi, *Prog. Histochem. Cytochem*. **1994**, *29*(2), 1.
[34] S. E. Armstrong, D. R. Bell, *Anal. Biochem*. **2002**, *308*(2), 255.
[35] C. Tolg, S. R. Hamilton, E. Zalinska, L. McCulloch, R. Amin, N. Akentieva, F. Winnik, R. Savani, D. J. Bagli, L. G. Luyt, M. K. Cowman, J. B. McCarthy, E. A. Turley, *Am. J. Pathol*. **2012**, *181*(4), 1250.
[36] X. Tian, J. Azpurua, C. Hine, A. Vaidya, M. Myakishev-Rempel, J. Ablaeva, Z. Mao, E. Nevo, V. Gorbunova, A. Seluanov, *Nature* **2013**, *499*(7458), 346.
[37] D. Del Marmol, S. Holtze, N. Kichler, A. Sahm, B. Bihin, V. Bourguignon, S. Dogné, K. Szafranski, T. B. Hildebrandt, B. Flamion, *Sci. Rep*. **2021**, *11*(1), 7951.
[38] H. Yuan, R. Amin, X. Ye, C. A. de la Motte, M. K. Cowman, *Anal. Biochem*. **2015**, *474*, 78.
[39] L. B. Dahl, I. M. S. Dahl, A. L. Børresen, *Biochem. Med. Metab. Biol*. **1986**, *35*(2), 219.
[40] A. Tengblad, U. B. G. Laurent, K. Lilja, R. N. P. Cahill, A. Engström-Laurent, J. R. R. Fraser, H. E. Hansson, T. C. Laurent, *Biochem. J*. **1986**, *236*(2), 521.

[41] S. E. Armstrong, D. R. Bell, *Am. J. Physiol. Heart Circ. Physiol*. **2002**, *283*(6), H2485.
[42] Y. Sasaki, M. Uzuki, K. Nohmi, H. Kitagawa, A. Kamataki, M. Komagamine, K. Murakami, T. Sawai, *Int. J. Rheum. Dis*. **2011**, *14*(4), 313.
[43] V. B. Lokeshwar, C. Obek, M. S. Soloway, N. L. Block, *Cancer Res*. **1997**, *57*(4), 773.
[44] E. J. Franzmann, G. L. Schroeder, W. J. Goodwin, D. T. Weed, P. Fisher, V. B. Lokeshwar, *Int. J. Cancer* **2003**, *106*(3), 438.
[45] L. Rauhala, L. Hämäläinen, P. Salonen, G. Bart, M. Tammi, S. Pasonen -Seppänen, R. Tammi, *J. Biol. Chem*. **2013**, *288*(25), 17999.
[46] V. B. Lokeshwar, D. Rubinowicz, G. L. Schroeder, E. Forgacs, J. D. Minna, N. L. Block, M. Nadji, B. L. Lokeshwar, *J. Biol. Chem*. **2001**, *276*(15), 11922.
[47] A. E. Decleves, N. Caron, V. Voisin, A. Legrand, N. Bouby, A. Kultti, M. I. Tammi, B. Flamion, *Nephrol. Dial. Transplant*. **2012**, *27*(10), 3771.
[48] M. K. Cowman, S. Matsuoka, *Carbohydr. Res*. **2005**, *340*(5), 791.
[49] M. K. Cowman, *Adv. Carbohydr. Chem. Biochem*. **2017**, *74*, 1.
[50] J. M. Guss, D. W. L. Hukins, P. J. C. Smith, W. T. Winter, S. Arnott, R. Moorhouse, D. A. Rees, *J. Mol. Biol*. **1975**, *95*(3), 359.
[51] W. T. Winter, P. J. C. Smith, S. Arnott, *J. Mol. Biol*. **1975**, *99*(2), 219.
[52] W. T. Winter, S. Arnott, *J. Mol. Biol*. **1977**, *117*(3), 761.
[53] J. K. Sheehan, E. D. T. Atkins, *Int. J. Biol. Macromol*. **1983**, *5*(4), 215.
[54] M. K. Cowman, D. Cozart, K. Nakanishi, E. A. Balazs, *Arch. Biochem. Biophys*. **1984**, *230*(1), 203.
[55] M. K. Cowman, D. M. Hittner, J. Feder-Davis, *Macromolecules* **1996**, *29*(8), 2894.
[56] M. K. Cowman, J. Feder-Davis, D. M. Hittner, *Macromolecules* **2001**, *34*(1), 110.
[57] F. Cavalieri, E. Chiessi, M. Paci, G. Paradossi, A. Flaibani, A. Cesàro, *Macromolecules* **2001**, *34*(1), 99.
[58] S. Letardi, G. La Penna, E. Chiessi, A. Perico, A. Cesàro, *Macromolecules* **2002**, *35*(1), 286.
[59] E. A. Balazs, *Fed. Proc*. **1958**, *17*(4), 1086.
[60] T. C. Laurent, M. Ryan, A. Pietruszkiewicz, *Biochim. Biophys. Acta* **1960**, *42*, 476.
[61] E. A. Balazs, *Univ. Mich. Med. Cent. J*. **1968**, 255.
[62] R. L. Cleland, *Arch. Biochem. Biophys*. **1977**, *180*(1), 57.
[63] R. L. Cleland, *Biopolymers* **1984**, *23*(4), 647.
[64] K. Hayashi, K. Tsutsumi, F. Nakajima, T. Norisuye, A. Teramoto, *Macromolecules* **1995**, *28*(11), 3824.
[65] K. Hayashi, K. Tsutsumi, T. Norisuye, A. Teramoto, *Polym. J*. **1996**, *28*(10), 922.
[66] R. E. Turner, P. Lin, M. K. Cowman, *Arch. Biochem. Biophys*. **1988**, *265*(2), 484.
[67] R. L. Cleland, J. L. Wang, *Biopolymers* **1970**, *9*(7), 799.
[68] E. Shimada, G. Matsumura, *J. Biochem*. **1975**, *78*(3), 513.
[69] M. K. Cowman, T. A. Schmidt, P. Raghavan, A. Stecco, *F1000Research* **2015**, *4*, 622.
[70] M. K. Cowman, *Polym. Adv. Technol*. **2017**, *28*(8), 1000.
[71] D. A. Gibbs, E. W. Merrill, K. A. Smith, E. A. Balazs, *Biopolymers* **1968**, *6*(6), 777.
[72] E. Fouissac, M. Milas, M. Rinaudo, *Macromolecules* **1993**, *26*(25), 6945.
[73] N. Berriaud, M. Milas, M. Rinaudo, *Int. J. Biol. Macromol*. **1994**, *16*(3), 137.
[74] M. Milas, M. Rinaudo, I. Roure, S. Al-Assaf, G. O. Phillips, P. A. Williams, *Biopolymers* **2001**, *59*(4), 191.
[75] W. Burchard, *Biomacromolecules* **2001**, *2*(2), 342.
[76] J. K. Sheehan, K. H. Gardner, E. D. T. Atkins, *J. Mol. Biol*. **1977**, *117*(1), 113.
[77] S. Arnott, A. K. Mitra, S. Raghunathan, *J. Mol. Biol*. **1983**, *169*(4), 861.
[78] J. H. Fessler, L. I. Fessler, *Proce. Natl. Acad. Sci*. **1966**, *56*(1), 141.
[79] J. E. Scott, C. Cummings, A. Brass, Y. Chen, *Biochem. J*. **1991**, *274*(Pt 3), 699.
[80] N. M. Hadler, R. R. Dourmashkin, M. V. Nermut, L. D. Williams, *Proc. Natl. Acad. Sci*. **1982**, *79*(2), 307.
[81] M. K. Cowman, M. Li, E. A. Balazs, *Biophys. J*. **1998**, *75*(4), 2030.
[82] M. K. Cowman, C. Spagnoli, D. Kudasheva, M. Li, A. Dyal, S. Kanai, E. A. Balazs, *Biophys. J*. **2005**, *88*(1), 590.
[83] T. C. Laurent, *Biophys. Chem*. **1995**, *57*(1), 7.
[84] T. C. Laurent, *Biochem. J*. **1964**, *93*(1), 106.
[85] S. Evanko, M. Tammi, R. Tammi, T. Wight, *Adv. Drug Deliv. Rev*. **2007**, *59*(13), 1351.
[86] W. Knudson, S. Ishizuka, K. Terabe, E. B. Askew, C. B. Knudson, *Matrix Biol*. **2019**, *78–79*, 32.
[87] H. Watanabe, *Am. J. Physiol. Cell Physiol*. **2022**, *322*(5), C967.
[88] R. L. Goldberg, B. P. Toole, *J. Cell Biol*. **1984**, *99*(6), 2114.
[89] S. Pasonen-Seppänen, J. M. T. Hyttinen, K. Rilla, T. Jokela, P. W. Noble, M. Tammi, R. Tammi, *Histochem. Cell Biol*. **2012**, *137*(1), 107.
[90] C. B. Knudson, *J. Cell Biol*. **1993**, *120*(3), 825.
[91] G. M. Lee, B. Johnstone, K. Jacobson, B. Caterson, *J. Cell Biol*. **1993**, *123*(6 Pt 2), 1899.
[92] L. T. McLane, P. Chang, A. Granqvist, H. Boehm, A. Kramer, J. Scrimgeour, J. E. Curtis, *Biophys. J*. **2013**, *104*(5), 986.
[93] P. S. Chang, L. T. McLane, R. Fogg, J. Scrimgeour, J. S. Temenoff, A. Granqvist, J. E. Curtis, *Biophys. J*. **2016**, *110*(12), 2739.
[94] H. Boehm, T. A. Mundinger, C. H. J. Boehm, V. Hagel, U. Rauch, J. P. Spatz, J. E. Curtis, *Soft Matter* **2009**, *5*(21), 4331.
[95] J. Scrimgeour, L. T. McLane, P. S. Chang, J. E. Curtis, *Biophys. J*. **2017**, *113*(11), 2316.
[96] A. J. Day, C. M. Milner, *Matrix Biol*. **2019**, *78–79*, 60.
[97] T. I. Morales, V. C. Hascall, *J. Biol. Chem*. **1988**, *263*(8), 3632.
[98] R. Stern, M. J. Jedrzejas, *Chem. Rev*. **2006**, *106*(3), 818.
[99] R. Stern, G. Kogan, M. J. Jedrzejas, L. Šoltés, *Biotechnol. Adv*. **2007**, *25*(6), 537.
[100] D. Hida, B. T. Danielson, C. B. Knudson, W. Knudson, *Matrix Biol*. **2015**, *48*, 42.
[101] L. Y. W. Bourguignon, P. A. Singleton, F. Diedrich, R. Stern, E. Gilad, *J. Biol. Chem*. **2004**, *279*(26), 26991.
[102] H. Yoshida, A. Nagaoka, A. Kusaka-Kikushima, M. Tobiishi, K. Kawabata, T. Sayo, S. Sakai, Y. Sugiyama, H. Enomoto, Y. Okada, S. Inoue, *Proc. Natl. Acad. Sci*. **2013**, *110*(14), 5612.
[103] Y. Yamaguchi, H. Yamamoto, Y. Tobisawa, F. Irie, *Matrix Biol*. **2019**, *78-79*, 139.
[104] H. Yamamoto, Y. Tobisawa, T. Inubushi, F. Irie, C. Ohyama, Y. Yamaguchi, *J. Biol. Chem*. **2017**, *292*(18), 7304.
[105] W. Ariyoshi, N. Takahashi, D. Hida, C. B. Knudson, W. Knudson, *Arthritis Rheum*. **2012**, *64*(1), 187.
[106] M. Li, L. Rosenfeld, R. E. Vilar, M. K. Cowman, *Arch. Biochem. Biophys*. **1997**, *341*(2), 245.
[107] L. Šoltés, G. Kogan, M. Stankovská, R. Mendichi, J. Rychlý, J. Schiller, P. Gemeiner, *Biomacromolecules* **2007**, *8*(9), 2697.
[108] K. L. Schwertfeger, M. K. Cowman, P. G. Telmer, E. A. Turley, J. B. McCarthy, *Front. Immunol*. **2015**, *6*, 236.
[109] A. C. Petrey, C. A. de la Motte, *Front. Immunol*. **2014**, *5*, 101.
[110] S. Albeiroti, A. Soroosh, C. A. de la Motte, *BioMed Res. Int*. **2015**, *2015*, 790203.
[111] P. Heldin, C. Y. Lin, C. Kolliopoulos, Y. H. Chen, S. S. Skandalis, *Matrix Biol*. **2019**, *78-79*, 100.
[112] T. Karalis, S. S. Skandalis, *Am. J. Physiol. Cell Physiol*. **2022**, *323*(1), C145.
[113] A. Peters, L. S. Sherman, *Int. J. Mol. Sci*. **2020**, *21*(17), 5988.
[114] R. D. Altman, V. Dasa, J. Takeuchi, *Cartilage* **2018**, *9*(1), 11.
[115] R. Altman, A. Bedi, A. Manjoo, F. Niazi, P. Shaw, P. Mease, *Cartilage* **2019**, *10*(1), 43.

[116] E. A. Balazs, P. A. Band, *Carbohydrate Chemistry, Biology and Medical Applications* (Eds: H. G. Garg, M. K. Cowman, C. A. Hales), Elsevier, Amsterdam **2008**, p. 311.
[117] G. Abatangelo, V. Vindigni, G. Avruscio, L. Pandis, P. Brun, *Cells* **2020**, *9*(7), 1743.
[118] K. Valachová, L. Šoltés, *Int. J. Mol. Sci.* **2021**, *22*(13), 7077.
[119] M. I. Tammi, S. Oikari, S. Pasonen-Seppänen, K. Rilla, P. Auvinen, R. H. Tammi, *Matrix Biol.* **2019**, *78-79*, 147.
[120] U. Hellman, M. G. Karlsson, A. Engström-Laurent, S. Cajander, L. Dorofte, C. Ahlm, C. Laurent, A. Blomberg, *J. Biol. Chem.* **2020**, *295*(45), 15418.
[121] N. Albtoush, A. C. Petrey, *Am. J. Physiol. Cell Physiol.* **2022**, *322*(6), C1037.
[122] C. M. McKee, M. B. Penno, M. Cowman, M. D. Burdick, R. M. Strieter, C. Bao, P. W. Noble, *J. Clin. Invest.* **1996**, *98*(10), 2403.
[123] K. A. Scheibner, M. A. Lutz, S. Boodoo, M. J. Fenton, J. D. Powell, M. R. Horton, *J. Immunol.* **2006**, *177*(2), 1272.
[124] K. R. Taylor, K. Yamasaki, K. A. Radek, A. D. Nardo, H. Goodarzi, D. Golenbock, B. Beutler, R. L. Gallo, *J. Biol. Chem.* **2007**, *282*(25), 18265.
[125] D. Jiang, J. Liang, P. W. Noble, *Physiol. Rev.* **2011**, *91*(1), 221.
[126] J. Monslow, P. Govindaraju, E. Puré, *Front. Immunol.* **2015**, *6*, 231.
[127] A. G. Tavianatou, Z. Piperigkou, C. Barbera, R. Beninatto, V. Masola, I. Caon, M. Onisto, M. Franchi, D. Galesso, N. K. Karamanos, *Matrix Biol. Plus* **2019**, *3*, 100008.
[128] A. Avenoso, G. Bruschetta, A. D'Ascola, M. Scuruchi, G. Mandraffino, R. Gullace, A. Saitta, S. Campo, G. M. Campo, *Arch. Biochem. Biophys.* **2019**, *663*, 228.
[129] J. M. Cyphert, C. S. Trempus, S. Garantziotis, *Int. J. Cell Biol.* **2015**, *2015*, 563818.
[130] D. B. Lyle, J. C. Breger, L. F. Baeva, J. C. Shallcross, C. N. Durfor, N. S. Wang, J. J. Langone, *J. Biomed. Mater. Res. A* **2010**, *94*(3), 893.
[131] Y. Dong, A. Arif, M. Olsson, V. Cali, B. Hardman, M. Dosanjh, M. Lauer, R. J. Midura, V. C. Hascall, K. L. Brown, P. Johnson, *Sci. Rep.* **2016**, *6*, 36928.
[132] B. Šafránková, M. Hermannová, K. Nešporová, V. Velebný, L. Kubala, *Int. J. Biol. Macromol.* **2018**, *107*(Pt A), 1.
[133] M. Olsson, L. Bremer, C. Aulin, H. E. Harris, *Innate Immun.* **2018**, *24*(2), 131.
[134] M. K. Cowman, C. Shortt, S. Arora, Y. Fu, J. Villavieja, J. Rathore, X. Huang, T. Rakshit, G. I. Jung, T. Kirsch, *Inflammation* **2019**, *42*(5), 1808.
[135] Z. Huang, C. Zhao, Y. Chen, J. A. Cowell, G. Wei, A. Kultti, L. Huang, C. B. Thompson, S. Rosengren, G. I. Frost, H. M. Shepard, *J. Immunol.* **2014**, *192*(11), 5285.
[136] Y. Kim, G. A. West, G. Ray, S. P. Kessler, A. C. Petrey, C. Fiocchi, C. McDonald, M. S. Longworth, L. E. Nagy, C. A. de la Motte, *Matrix Biol.* **2018**, *66*, 93.
[137] D. R. Hill, S. P. Kessler, H. K. Rho, M. K. Cowman, C. A. de la Motte, *J. Biol. Chem.* **2012**, *287*(36), 30610.
[138] C. Underhill, A. Dorfman, *Exp. Cell Res.* **1978**, *117*(1), 155.
[139] C. B. Underhill, B. P. Toole, *J. Cell Biol.* **1979**, *82*(2), 475.
[140] C. B. Underhill, B. P. Toole, *J. Biol. Chem.* **1980**, *255*(10), 4544.
[141] C. B. Underhill, B. P. Toole, *Exp. Cell Res.* **1981**, *131*(2), 419.
[142] C. B. Underhill, *J. Cell Sci.* **1982**, *56*, 177.
[143] C. B. Underhill, G. Chi-Rosso, B. P. Toole, *J. Biol. Chem.* **1983**, *258*(13), 8086.
[144] L. J. Picker, M. Nakache, E. C. Butcher, *J. Cell Biol.* **1989**, *109*(2), 927.
[145] B. F. Flanagan, R. Dalchau, A. K. Allen, A. S. Daar, J. W. Fabre, *Immunology* **1989**, *67*(2), 167.
[146] Y. Nishida, C. B. Knudson, W. Knudson, *Modern Rheumatol.* **2003**, *13*(1), 62.
[147] I. Stamenkovic, M. Amiot, J. M. Pesando, B. Seed, *Cell* **1989**, *56*(6), 1057.
[148] D. F. Zhou, J. F. Ding, L. J. Picker, R. F. Bargatze, E. C. Butcher, D. V. Goeddel, *J. Immunol.* **1989**, *143*(10), 3390.
[149] C. Nottenburg, G. Rees, T. St John, *Proc. Natl. Acad. Sci.* **1989**, *86*(21), 8521.
[150] G. R. Screaton, M. V. Bell, D. G. Jackson, F. B. Cornelis, U. Gerth, J. I. Bell, *Proc. Natl. Acad. Sci.* **1992**, *89*(24), 12160.
[151] M. V. Bell, A. E. Cowper, M. P. Lefranc, J. I. Bell, G. R. Screaton, *Mol. Cell. Biol.* **1998**, *18*(10), 5930.
[152] J. Lesley, R. Hyman, *Front. Biosci.* **1998**, *3*, d616.
[153] C. B. Underhill, A. L. Thurn, B. E. Lacy, *J. Biol. Chem.* **1985**, *260*(13), 8128.
[154] C. B. Underhill, S. J. Green, P. M. Comoglio, G. Tarone, *J. Biol. Chem.* **1987**, *262*(27), 13142.
[155] L. A. Goldstein, D. F. H. Zhou, L. J. Picker, C. N. Minty, R. F. Bargatze, J. F. Ding, E. C. Butcher, *Cell* **1989**, *56*(6), 1063.
[156] S. P. Thankamony, W. Knudson, *J. Biol. Chem.* **2006**, *281*(45), 34601.
[157] T. Murai, *Front. Immunol.* **2015**, *6*, 420.
[158] D. G. Jackson, J. I. Bell, R. Dickinson, J. Timans, J. Shields, N. Whittle, *J. Cell Biol.* **1995**, *128*(4), 673.
[159] K. L. Bennett, B. Modrell, B. Greenfield, A. Bartolazzi, I. Stamenkovic, R. Peach, D. G. Jackson, F. Spring, A. Aruffo, *J. Cell Biol.* **1995**, *131*(6 Pt 1), 1623.
[160] R. Peach, D. Hollenbaugh, I. Stamenkovic, A. Aruffo, *J. Cell Biol.* **1993**, *122*(1), 257.
[161] J. Bajorath, B. Greenfield, S. B. Munro, A. J. Day, A. Aruffo, *J. Biol. Chem.* **1998**, *273*(1), 338.
[162] P. Teriete, S. Banerji, M. Noble, C. D. Blundell, A. J. Wright, A. R. Pickford, E. Lowe, D. J. Mahoney, M. I. Tammi, J. D. Kahmann, I. D. Campbell, A. J. Day, D. G. Jackson, *Mol. Cell* **2004**, *13*(4), 483.
[163] N. M. English, J. F. Lesley, R. Hyman, *Cancer Res.* **1998**, *58*(16), 3736.
[164] S. Banerji, A. J. Wright, M. Noble, D. J. Mahoney, I. D. Campbell, A. J. Day, D. G. Jackson, *Nat. Struct. Mol. Biol.* **2007**, *14*(3), 234.
[165] M. Takeda, H. Terasawa, M. Sakakura, Y. Yamaguchi, M. Kajiwara, H. Kawashima, M. Miyasaka, I. Shimada, *J. Biol. Chem.* **2003**, *278*(44), 43550.
[166] M. Takeda, S. Ogino, R. Umemoto, M. Sakakura, M. Kajiwara, K. N. Sugahara, H. Hayasaka, M. Miyasaka, H. Terasawa, I. Shimada, *J. Biol. Chem.* **2006**, *281*(52), 40089.
[167] S. Ogino, N. Nishida, R. Umemoto, M. Suzuki, M. Takeda, H. Terasawa, J. Kitayama, M. Matsumoto, H. Hayasaka, M. Miyasaka, I. Shimada, *Structure* **2010**, *18*(5), 649.
[168] A. J. Favreau, C. E. Faller, O. Guvench, *Biophys. J.* **2013**, *105*(5), 1217.
[169] O. Guvench, *Molecules* **2022**, *27*(21), 7276.
[170] L. A. Johnson, D. G. Jackson, *Cells* **2021**, *10*(8), 2061.
[171] T. Suzuki, M. Suzuki, S. Ogino, R. Umemoto, N. Nishida, I. Shimada, *Proc. Natl. Acad. Sci.* **2015**, *112*(22), 6991.
[172] M. Lintuluoto, Y. Horioka, S. Hongo, J. M. Lintuluoto, Y. Fukunishi, *ACS Omega* **2021**, *6*(12), 8045.
[173] J. Lesley, N. English, A. Perschl, J. Gregoroff, R. Hyman, *J. Exp. Med.* **1995**, *182*(2), 431.
[174] J. Vuorio, J. Škerlová, M. Fábry, V. Veverka, I. Vattulainen, P. Řezáčová, H. Martinez-Seara, *Sci. Rep.* **2021**, *11*(1), 5239.
[175] S. Katoh, T. Miyagi, H. Taniguchi, Y. Matsubara, J. Kadota, A. Tominaga, P. W. Kincade, S. Matsukura, S. Kohno, *J. Immunol.* **1999**, *162*(9), 5058.
[176] K. Gee, M. Kozlowski, A. Kumar, *J. Biol. Chem.* **2003**, *278*(39), 37275.
[177] H. Kellett-Clarke, M. Stegmann, A. N. Barclay, C. Metcalfe, *PLoS One* **2015**, *10*(9), e0138137.
[178] J. Lesley, V. C. Hascall, M. Tammi, R. Hyman, *J. Biol. Chem.* **2000**, *275*(35), 26967.

[179] J. Lesley, R. Hyman, *Eur. J. Immunol.* **1992**, *22*(10), 2719.
[180] J. Lesley, P. W. Kincade, R. Hyman, *Eur. J. Immunol.* **1993**, *23*(8), 1902.
[181] J. Lesley, N. Howes, A. Perschl, R. Hyman, *J. Exp. Med.* **1994**, *180*(1), 383.
[182] D. Liu, M. S. Sy, *J. Exp. Med.* **1996**, *183*(5), 1987.
[183] D. Liu, M. S. Sy, *J. Immunol.* **1997**, *159*(6), 2702.
[184] A. Perschl, J. Lesley, N. English, R. Hyman, I. S. Trowbridge, *J. Cell Sci.* **1995**, *108*(Pt 3), 1033.
[185] S. Banerji, B. R. S. Hide, J. R. James, M. E. M. Noble, D. G. Jackson, *J. Biol. Chem.* **2010**, *285*(14), 10724.
[186] M. Hartmann, L. M. Parra, A. Ruschel, C. Lindner, H. Morrison, A. Herrlich, P. Herrlich, *J. Biol. Chem.* **2015**, *290*(28), 17041.
[187] G. V. Dubacheva, T. Curk, R. Auzély-Velty, D. Frenkel, R. P. Richter, *Proc. Natl. Acad. Sci.* **2015**, *112*(18), 5579.
[188] A. Aruffo, I. Stamenkovic, M. Melnick, C. B. Underhill, B. Seed, *Cell* **1990**, *61*(7), 1303.
[189] P. M. Wolny, S. Banerji, C. Gounou, A. R. Brisson, A. J. Day, D. G. Jackson, R. P. Richter, *J. Biol. Chem.* **2010**, *285*(39), 30170.
[190] S. Mizrahy, S. R. Raz, M. Hasgaard, H. Liu, N. Soffer-Tsur, K. Cohen, R. Dvash, D. Landsman-Milo, M. G. E. G. Bremer, S. M. Moghimi, D. Peer, *J. Controlled Release* **2011**, *156*(2), 231.
[191] L. Y. Bourguignon, V. B. Lokeshwar, X. Chen, W. G. Kerrick, *J. Immunol.* **1993**, *151*(12), 6634.
[192] C. Yang, M. Cao, H. Liu, Y. He, J. Xu, Y. Du, Y. Liu, W. Wang, L. Cui, J. Hu, F. Gao, *J. Biol. Chem.* **2012**, *287*(51), 43094.
[193] L. Zhuo, A. Kanamori, R. Kannagi, N. Itano, J. Wu, M. Hamaguchi, N. Ishiguro, K. Kimata, *J. Biol. Chem.* **2006**, *281*(29), 20303.
[194] W. Lawrance, S. Banerji, A. J. Day, S. Bhattacharjee, D. G. Jackson, *J. Biol. Chem.* **2016**, *291*(15), 8014.
[195] S. Banerji, W. Lawrance, C. Metcalfe, D. C. Briggs, A. Yamauchi, O. Dushek, P. A. van der Merwe, A. J. Day, D. G. Jackson, *J. Biol. Chem.* **2016**, *291*(48), 25004.
[196] S. Tsukita, S. Yonemura, *J. Biol. Chem.* **1999**, *274*(49), 34507.
[197] T. Mori, K. Kitano, S. Terawaki, R. Maesaki, Y. Fukami, T. Hakoshima, *J. Biol. Chem.* **2008**, *283*(43), 29602.
[198] T. Jokela, S. Oikari, P. Takabe, K. Rilla, R. Kärnä, M. Tammi, R. Tammi, *J. Biol. Chem.* **2015**, *290*(19), 12379.
[199] W. Knudson, D. J. Aguiar, Q. Hua, C. B. Knudson, *Exp. Cell Res.* **1996**, *228*(2), 216.
[200] S. A. Freeman, A. Vega, M. Riedl, R. F. Collins, P. P. Ostrowski, E. C. Woods, C. R. Bertozzi, M. I. Tammi, D. S. Lidke, P. Johnson, S. Mayor, K. Jaqaman, S. Grinstein, *Cell* **2018**, *172*(1–2), 305.
[201] A. R. Vega, S. A. Freeman, S. Grinstein, K. Jaqaman, *Biophys. J.* **2018**, *114*(5), 1018.
[202] P. Sil, N. Mateos, S. Nath, S. Buschow, C. Manzo, K. G. N. Suzuki, T. Fujiwara, A. Kusumi, M. F. Garcia-Parajo, S. Mayor, *Mol. Biol. Cell* **2020**, *31*(7), 561.
[203] T. A. Stanly, M. Fritzsche, S. Banerji, D. Shrestha, F. Schneider, C. Eggeling, D. G. Jackson, *J. Biol. Chem.* **2020**, *295*(15), 5036.
[204] S. J. Neame, C. R. Uff, H. Sheikh, S. C. Wheatley, C. M. Isacke, *J. Cell Sci.* **1995**, *108*(Pt 9), 3127.
[205] A. C. Midgley, M. Rogers, M. B. Hallett, A. Clayton, T. Bowen, A. O. Phillips, R. Steadman, *J. Biol. Chem.* **2013**, *288*(21), 14824.
[206] S. Donatello, I. S. Babina, L. D. Hazelwood, A. D. K. Hill, I. R. Nabi, A. M. Hopkins, *Am. J. Pathol.* **2012**, *181*(6), 2172.
[207] T. Murai, Y. Maruyama, K. Mio, H. Nishiyama, M. Suga, C. Sato, *J. Biol. Chem.* **2011**, *286*(3), 1999.
[208] T. Murai, C. Sato, M. Sato, H. Nishiyama, M. Suga, K. Mio, H. Kawashima, *J. Cell Sci.* **2013**, *126*(Pt 15), 3284.
[209] A. K. Saha, P. Osmulski, S. F. Dallo, M. Gaczynska, T. H. M. Huang, A. K. Ramasubramanian, *Biophys. J.* **2017**, *112*(7), 1481.
[210] L. Y. Bourguignon, E. L. Kalomiris, V. B. Lokeshwar, *J. Biol. Chem.* **1991**, *266*(18), 11761.
[211] I. S. Babina, E. A. McSherry, S. Donatello, A. D. Hill, A. M. Hopkins, *Breast Cancer Res.* **2014**, *16*(1), R19.
[212] B. Shao, T. Yago, H. Setiadi, Y. Wang, P. Mehta-D'souza, J. Fu, P. R. Crocker, W. Rodgers, L. Xia, R. P. McEver, *Proc. Natl. Acad. Sci.* **2015**, *112*(28), 8661.
[213] N. Sasaki, Y. Itakura, M. Toyoda, *Stem Cell Res. Ther.* **2017**, *8*(1), 81.
[214] E. Kalomiris, L. Bourguignon, *J. Cell. Biol.* **1988**, *106*(2), 319.
[215] V. B. Lokeshwar, N. Fregien, L. Y. Bourguignon, *J. Cell Biol.* **1994**, *126*(4), 1099.
[216] R. M. L. Simpson, A. Wells, D. Thomas, P. Stephens, R. Steadman, A. Phillips, *Am. J. Pathol.* **2010**, *176*(3), 1215.
[217] S. Meran, D. D. Luo, R. Simpson, J. Martin, A. Wells, R. Steadman, A. O. Phillips, *J. Biol. Chem.* **2011**, *286*(20), 17618.
[218] J. Martin, A. Midgley, S. Meran, E. Woods, T. Bowen, A. O. Phillips, R. Steadman, *J. Biol. Chem.* **2016**, *291*(26), 13789.
[219] L. Mellor, C. B. Knudson, D. Hida, E. B. Askew, W. Knudson, *J. Biol. Chem.* **2013**, *288*(36), 25838.
[220] I. Okamoto, Y. Kawano, D. Murakami, T. Sasayama, N. Araki, T. Miki, A. J. Wong, H. Saya, *J. Cell Biol.* **2001**, *155*(5), 755.
[221] S. Lammich, M. Okochi, M. Takeda, C. Kaether, A. Capell, A. K. Zimmer, D. Edbauer, J. Walter, H. Steiner, C. Haass, *J. Biol. Chem.* **2002**, *277*(47), 44754.
[222] J. Cichy, E. Puré, *J. Cell Biol.* **2003**, *161*(5), 839.
[223] I. Okamoto, Y. Kawano, H. Tsuiki, J. Sasaki, M. Nakao, M. Matsumoto, M. Suga, M. Ando, M. Nakajima, H. Saya, *Oncogene* **1999**, *18*(7), 1435.
[224] S. Terawaki, K. Kitano, M. Aoyama, T. Mori, T. Hakoshima, *Genes Cells* **2015**, *20*(10), 847.
[225] H. Mori, T. Tomari, N. Koshikawa, M. Kajita, Y. Itoh, H. Sato, H. Tojo, I. Yana, M. Seiki, *EMBO J.* **2002**, *21*(15), 3949.
[226] N. Suenaga, H. Mori, Y. Itoh, M. Seiki, *Oncogene* **2005**, *24*(5), 859.
[227] M. Kajita, Y. Itoh, T. Chiba, H. Mori, A. Okada, H. Kinoh, M. Seiki, *J. Cell Biol.* **2001**, *153*(5), 893.
[228] H. Nakamura, N. Suenaga, K. Taniwaki, H. Matsuki, K. Yonezawa, M. Fujii, Y. Okada, M. Seiki, *Cancer Res.* **2004**, *64*(3), 876.
[229] O. Nagano, H. Saya, *Cancer Sci.* **2004**, *95*(12), 930.
[230] O. Nagano, D. Murakami, D. Hartmann, B. de Strooper, P. Saftig, T. Iwatsubo, M. Nakajima, M. Shinohara, H. Saya, *J. Cell Biol.* **2004**, *165*(6), 893.
[231] K. N. Sugahara, T. Murai, H. Nishinakamura, H. Kawashima, H. Saya, M. Miyasaka, *J. Biol. Chem.* **2003**, *278*(34), 32259.
[232] K. N. Sugahara, T. Hirata, H. Hayasaka, R. Stern, T. Murai, M. Miyasaka, *J. Biol. Chem.* **2006**, *281*(9), 5861.
[233] E. A. Turley, *Biochem. Biophys. Res. Commun.* **1982**, *108*(3), 1016.
[234] C. A. Maxwell, J. J. Keats, M. Crainie, X. Sun, T. Yen, E. Shibuya, M. Hendzel, G. Chan, L. M. Pilarski, *Mol. Biol. Cell* **2003**, *14*(6), 2262.
[235] Z. He, L. Mei, M. Connell, C. A. Maxwell, *Cells* **2020**, *9*(4), 819.
[236] C. Meier, A. Spitschak, K. Abshagen, S. Gupta, J. M. Mor, O. Wolkenhauer, J. Haier, B. Vollmar, V. Alla, B. M. Pützer, *J. Pathol.* **2014**, *234*(3), 351.
[237] J. A. Hinneh, J. L. Gillis, N. L. Moore, L. M. Butler, M. M. Centenera, *Front. Oncol.* **2022**, *12*, 982231.
[238] A. Parnigoni, M. Viola, E. Karousou, S. Rovera, C. Giaroni, A. Passi, D. Vigetti, *Am. J. Physiol. Cell Physiol.* **2022**, *323*(2), C505.
[239] C. Wang, J. Entwistle, G. Hou, Q. Li, E. A. Turley, *Gene* **1996**, *174*(2), 299.
[240] J. Entwistle, S. Zhang, B. Yang, C. Wong, Q. Li, C. L. Hall, J. A. M. Mowat, A. H. Greenberg, E. A. Turley, *Gene* **1995**, *163*(2), 233.
[241] C. Fieber, R. Plug, J. Sleeman, P. Dall, H. Ponta, M. Hofmann, *Gene* **1999**, *226*(1), 41.
[242] A. Filaquier, P. Marin, M. L. Parmentier, J. Villeneuve, *Curr. Opin. Cell Biol.* **2022**, *75*, 102072.
[243] A. S. Menko, A. Romisher, J. L. Walker, *Front. Cell. Dev. Biol.* **2022**, *10*, 862423.
[244] A. Zaman, Z. Cui, J. P. Foley, H. Zhao, P. C. Grimm, H. M. DeLisser, R. C. Savani, *Am. J. Respir. Cell Mol. Biol.* **2005**, *33*(5), 447.

[245] M. Slevin, J. Krupinski, J. Gaffney, S. Matou, D. West, H. Delisser, R. C. Savani, S. Kumar, *Matrix Biol*. **2007**, *26*(1), 58.
[246] Y. Leng, A. Abdullah, M. K. Wendt, S. Calve, *Matrix Biol*. **2019**, *78-79*, 236.
[247] J. P. Foley, D. Lam, H. Jiang, J. Liao, N. Cheong, T. M. McDevitt, A. Zaman, J. R. Wright, R. C. Savani, *J. Biol. Chem*. **2012**, *287*(44), 37406.
[248] F. Gao, C. X. Yang, W. Mo, Y. W. Liu, Y. Q. He, *Clin. Invest. Med*. **2008**, *31*(3), E106.
[249] E. A. Turley, L. Austen, K. Vandeligt, C. Clary, *J. Cell Biol*. **1991**, *112*(5), 1041.
[250] R. C. Savani, C. Wang, B. Yang, S. Zhang, M. G. Kinsella, T. N. Wight, R. Stern, D. M. Nance, E. A. Turley, *J. Clin. Invest*. **1995**, *95*(3), 1158.
[251] A. Hauser-Kawaguchi, L. G. Luyt, E. Turley, *Matrix Biol*. **2019**, *78-79*, 346.
[252] Y. Akiyama, S. Jung, B. Salhia, S. Lee, S. Hubbard, M. Taylor, T. Mainprize, K. Akaishi, W. van Furth, J. T. Rutka, *J. Neuro-Oncol*. **2001**, *53*(2), 115.
[253] R. C. Savani, G. Hou, P. Liu, C. Wang, E. Simons, P. C. Grimm, R. Stern, A. H. Greenberg, H. M. DeLisser, N. Khalil, *Am. J. Respir. Cell Mol. Biol*. **2000**, *23*(4), 475.
[254] K. J. Till, M. Zuzel, J. C. Cawley, *Cancer Res*. **1999**, *59*(17), 4419.
[255] J. Wang, D. Li, W. Shen, W. Sun, R. Gao, P. Jiang, L. Wang, Y. Liu, Y. Chen, W. Zhou, R. Wang, R. Xiang, D. Stupack, N. Luo, *Anat. Rec*. **2020**, *303*(9), 2344.
[256] X. B. Cheng, S. Wang, H. Yang, H. Tong, G. Shi, L. Wu, J. Zhou, L. Shi, H. Li, S. Ren, Y. Zhou, N. Sato, *Oncol. Lett*. **2020**, *20*(5), 199.
[257] C. Hardwick, K. Hoare, R. Owens, H. Hohn, M. Hook, D. Moore, V. Cripps, L. Austen, D. Nance, E. Turley, *J. Cell Biol*. **1992**, *117*(6), 1343.
[258] M. Hofmann, C. Fieber, V. Assmann, M. Gottlicher, J. Sleeman, R. Plug, N. Howells, O. von Stein, H. Ponta, P. Herrlich, *J. Cell Sci*. **1998**, *111*(Pt 12), 1673.
[259] C. L. Hall, B. Yang, X. Yang, S. Zhang, M. Turley, S. Samuel, L. A. Lange, C. Wang, G. D. Curpen, R. C. Savani, A. H. Greenberg, E. A. Turley, *Cell* **1995**, *82*(1), 19.
[260] Y. C. N. Du, C. K. Chou, D. S. Klimstra, H. Varmus, *Proc. Natl. Acad. Sci*. **2011**, *108*(40), 16753.
[261] S. Choi, D. Wang, X. Chen, L. H. Tang, A. Verma, Z. Chen, B. J. Kim, L. Selesner, K. Robzyk, G. Zhang, S. Pang, T. Han, C. S. Chan, T. J. Fahey, O. Elemento, Y. C. N. Du, *Mol. Cancer* **2019**, *18*(1), 92.
[262] D. Nikitovic, K. Kouvidi, N. K. Karamanos, G. N. Tzanakakis, *BioMed Res. Int*. **2013**, *2013*, 929531.
[263] J. Jumper, R. Evans, A. Pritzel, T. Green, M. Figurnov, O. Ronneberger, K. Tunyasuvunakool, R. Bates, A. Žídek, A. Potapenko, A. Bridgland, C. Meyer, S. A. A. Kohl, A. J. Ballard, A. Cowie, B. Romera-Paredes, S. Nikolov, R. Jain, J. Adler, T. Back, S. Petersen, D. Reiman, E. Clancy, M. Zielinski, M. Steinegger, M. Pacholska, T. Berghammer, S. Bodenstein, D. Silver, O. Vinyals, A. W. Senior, K. Kavukcuoglu, P. Kohli, D. Hassabis, *Nature* **2021**, *596*(7873), 583.
[264] M. Varadi, S. Anyango, M. Deshpande, S. Nair, C. Natassia, G. Yordanova, D. Yuan, O. Stroe, G. Wood, A. Laydon, A. Žídek, T. Green, K. Tunyasuvunakool, S. Petersen, J. Jumper, E. Clancy, R. Green, A. Vora, M. Lutfi, M. Figurnov, A. Cowie, N. Hobbs, P. Kohli, G. Kleywegt, E. Birney, D. Hassabis, S. Velankar, *Nucleic Acids Res*. **2022**, *50*(D1), D439.
[265] V. Assmann, D. Jenkinson, J. F. Marshall, I. R. Hart, *J. Cell Sci*. **1999**, *112*(Pt 22), 3943.
[266] E. Turley, D. Moore, *Biochem. Biophys. Res. Commun*. **1984**, *121*(3), 808.
[267] E. A. Turley, D. Moore, L. J. Hayden, *Biochemistry* **1987**, *26*(11), 2997.
[268] E. A. Turley, L. Austen, D. Moore, K. Hoare, *Exp. Cell Res*. **1993**, *207*(2), 277.
[269] F. Chen, X. Zhu, J. Zheng, T. Xu, K. Wu, C. Ru, *Math. Biosci. Eng*. **2020**, *17*(3), 2150.
[270] A. Minato, Y. Kudo, H. Noguchi, S. Kohi, Y. Hasegawa, N. Sato, K. Hirata, N. Fujimoto, *Cancer Genom. Proteom*. **2023**, *20*(2), 203.
[271] Y. Goueffic, C. Guilluy, P. Guerin, P. Patra, P. Pacaud, G. Loirand, *Cardiovasc. Res*. **2006**, *72*(2), 339.
[272] S. Twarock, M. I. Tammi, R. C. Savani, J. W. Fischer, *J. Biol. Chem*. **2010**, *285*(30), 23276.
[273] V. Mele, L. Sokol, V. H. Kölzer, D. Pfaff, M. G. Muraro, I. Keller, Z. Stefan, I. Centeno, L. M. Terracciano, H. Dawson, I. Zlobec, G. Iezzi, A. Lugli, *Oncotarget* **2017**, *8*(41), 70617.
[274] B. Yang, L. Zhang, E. A. Turley, *J. Biol. Chem*. **1993**, *268*(12), 8617.
[275] M. R. Ziebell, G. D. Prestwich, *J. Comput.-Aided Mol. Des*. **2004**, *18*(10), 597.
[276] V. Assmann, J. F. Marshall, C. Fieber, M. Hofmann, I. R. Hart, *J. Cell Sci*. **1998**, *111*(Pt 12), 1685.
[277] E. A. Turley, P. W. Noble, L. Y. W. Bourguignon, *J. Biol. Chem*. **2002**, *277*(7), 4589.
[278] A. M. Carvalho, D. Soares da Costa, R. L. Reis, I. Pashkuleva, *Acta Biomater*. **2022**, *146*, 187.
[279] A. M. Carvalho, D. Soares da Costa, P. M. R. Paulo, R. L. Reis, I. Pashkuleva, *Acta Biomater*. **2021**, *119*, 114.
[280] S. R. Hamilton, S. F. Fard, F. F. Paiwand, C. Tolg, M. Veiseh, C. Wang, J. B. McCarthy, M. J. Bissell, J. Koropatnick, E. A. Turley, *J. Biol. Chem*. **2007**, *282*(22), 16667.

How to cite this article: M. K. Cowman, E. A. Turley, *Proteoglycan Res*. **2023**, *1*, e4. https://doi.org/10.1002/pgr2.4